PERFORMANCE IMPROVEMENT IN S-DUCT DIFFUSERS WITH BOUNDARY LAYER FENCES AND VORTEX GENERATORS

by
SOURABH MISHRA

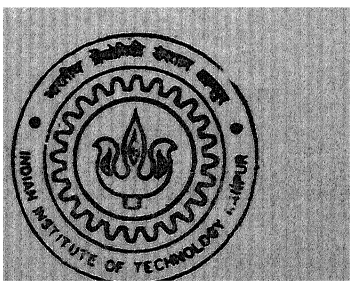

DEPARTMENT OF AEROSPACE ENGINEERING
INDIAN INSTITUTE OF TECHNOLOGY KANPUR

February, 2000

PERFORMANCE IMPROVEMENT IN S-DUCT DIFFUSERS WITH BOUNDARY LAYER FENCES AND VORTEX GENERATORS

A Thesis Submitted
in Partial Fulfilment of the Requirements
for the Degree of
MASTER OF TECHNOLOGY

by
Sourabh Mishra

to the

Department of Aerospace Engineering
Indian Institute of Technology Kanpur
February 2000

CERTIFICATE

This is to certify that the work contained in the thesis entitled "**Performance improvement in S-duct diffuser with boundary layer fences and vortex generators**" is a record of the work carried out by Mr Sourabh Mishra under my supervision and that it has not been submitted elsewhere for award of a degree

(R K Sullerey)

Professor

Department of Aerospace Engineering

Indian Institute of Technology Kanpur

Name Sourabh Mishra

Roll No 980116

Thesis Title Performance Improvement in S-duct Diffusers With Boundary Layer Fences and Vortex Generators

Thesis Supervisor Dr R K Sullerey

Professor

Department of Aerospace Engineering

I I T Kanpur, India

ABSTRACT

An experimental investigation was undertaken to study the effect of boundary layer fences and vortex generators (wishbone type) on the performance of two-dimensional S-duct diffusers having rectangular cross-section Experiments were performed in an open-circuit wind tunnel at a Reynolds number of 7.8×10^5 The various configurations tested were obtained by

1) Varying fence height,

2) Varying fence location and

3) Using various combinations of fences and vortex generators

The radius of curvature to half inlet width ratio for the two diffusers were 6 and 4 respectively and hence the two were subjected to different curvature effects The centerline arc length and area ratio was same for the two diffusers Detailed measurements including total pressure and velocity measurements, surface static

pressure, skin friction and boundary layer measurements were taken These results are reported here along with static pressure rise, distortion coefficient and total pressure loss coefficient determined from the experimental data The results indicate that a substantial improvement in diffuser performance is possible with proper use of fences and vortex generators In both the diffusers, the configuration employing only fences gave the best results The improvement in C_p value for the first diffuser was 18 6% and for the second diffuser it was 12 3% The distortion coefficient improved from 0 662 to 0 588 in the first diffuser and from 0 786 to 0 707 in the second one The results also indicate a decrease in total pressure losses with the use of fences and vortex generator Three-dimensional flow measurements using five-hole conical probe indicated a considerable reduction in secondary flows with fences

ACKNOWLEDGEMENTS

I wish to express my profound gratitude to Prof R K Sullerey for his invaluable guidance, constant encouragement and advice at every stage of my thesis that made this work possible

I feel extremely thankful to Mr V C Shrivastava for assisting me in various fabrication jobs throughout my work

I would like to convey my special regards to all my friends for the help and encouragement they provided during the course of my thesis

My special thanks to our workshop employees who fabricated the various setups required for this work

Finally I must express my deepest sense of gratitude to my family members for their loving care and encouragement

CONTENTS

NOMENCLATURE

AR = area ratio

C_p = pressure coefficient

C_f = skin fiction coefficient

D_c = distortion coefficient

h = diffuser height

l = duct centerline length

p = static pressure

p_o = total pressure

p_{rec} = total pressure recovery ratio(outlet to inlet)

r = inlet half width

R = duct centerline radius of curvature

Re = Reynolds number

s = distance along the duct centerline

Z = coordinate along diffuser height

Y = coordinate along duct centerline radius

ρ = fluid density

V = fluid velocity

VR = Vortex generator

ω = total pressure loss coefficient

P_i = pressure at i^{th} port, where $i = 1,2, \quad ,5$

P_{oi} = local total pressure (with reference to reference pressure used)

$P_{\infty i}$ = local static pressure

C_o = total pressure coefficient

C_q = dynamic pressure coefficient

α = pitch angle

β = yaw angle

For 5-hole probe

Subscript

max = maximum value

min = minimum value

av = average value

1,2 = notations for inlet and exit planes

ref = inlet plane (reference)

∞ = free stream value

List of Figures

Fig 15(b) Velocity distribution at the diffuser (R/r=4) exit with fences

Fig 15(c) Velocity distribution at the diffuser (R/r=4) exit with VG

Fig 15(d) Velocity distribution at the diffuser (R/r=4) exit with fences and VG

Fig 16 ω distribution inflection plane (R/r=4)

Fig 17(a) ω distribution at diffuser (R/r=4) exit

Fig 17(b) ω distribution at diffuser (R/r=4) exit with fences

Fig 17(c) ω distribution at diffuser (R/r=4) exit with VG

Fig 17(d) ω distribution at diffuser (R/r=4) exit with fences and VG

Fig 18 Transverse velocity distribution at diffuser (R/r=4) inflection plane

Fig 19(a) Transverse velocity distribution at diffuser (R/r=4) exit

Fig 19(b) Transverse velocity distribution at diffuser (R/r=4) exit with fences

Fig 20 Comparison of centerline C_p distribution for the two diffusers

Fig 21 Cp distribution at the diffuser (R/r=4) exit

CHAPTER 1

Introduction

An S-shaped diffuser is an essential feature of a combat aircraft inlet system A primary purpose of the S-duct is to convey air from the wing or fuselage intake to engine compressor The deceleration of flow needs to be so conducted as to obtain high static pressure and uniform flow at the diffuser outlet with minimum total pressure loss A short duct is desired because of space and aircraft weight considerations, resulting in high degrees of centerline curvature The centerline curvature gives rise to streamline curvature causing cross-stream pressure gradients. These cross-stream pressure gradients impart a transverse or cross flow velocity, known as secondary flow, to the fluid within the boundary layer. The axial development of these secondary flows in counter-rotating vortices at the duct exit is responsible for good deal of flow non-uniformity at the engine face. These secondary flows convect the low energy boundary layer fluid from duct surface to the center of the duct, creating highly non-uniform cross-stream total pressure profiles Additionally, streamwise adverse pressure gradient results from increasing cross-sectional area The combined effect may result in a region of flow separation, leading to increased total pressure non-uniformity (i.e distortion) and total pressure loss at the duct exit This flow blockage reduces the total pressure recovery of the duct

Diffusion occurs locally when flow approaches a bend in a constant area curved duct The potential flow model requires that flow decelerates on the inside wall and accelerates on the outside wall. Therefore diffusion occurs approaching the outside of the bend and leaving the inside of a bend and these are the locations were

diffusion, further increasing the probability of flow separation

Generation of secondary flow In a curved flow, to make the free stream fluid follow a curved path there must be a pressure gradient parallel to the surface but normal to the streamline direction The magnitude of this pressure gradient is sufficient to produce the centripetal acceleration of the free stream, V^2/R, where R is the radius of curvature of the free stream. The flow inside the boundary layer has lower velocity, $v<V$, and the pressure gradient set up by free stream exceeds that needed to make the flow follow the same radius of curvature as that of free stream The boundary layer fluid thus follows a tighter curve of smaller radius, generating cross-flow velocity components, known as secondary flow, perpendicular to free-stream direction

The boundary layer fluid tends to move outwards from outside of the bend towards the inside The energetic particles are displaced from the near wall and so low energy fluid accumulates near the inside of the bend, which is unable to withstand the adverse pressure gradient

A well-designed diffusing duct should efficiently decelerate the incoming flow, over a wide range of incoming conditions, without the occurrence of streamwise separation. Moreover, to achieve appropriate engine performance, it must incur minimal total pressure losses and deliver nearly uniform flow with small transverse velocity components at the engine compressor entrance The flow conditions emerging from the duct plays a crucial role in the design of downstream elements like compressor, combustion chamber etc. Instances have occurred of engine surging in flight because the angle of swirl, in absence of inlet guide vanes, has been sufficient for compressor stall

ducts Amongst the military aircraft the F-16, F-18, LCA and many others use S-shaped diffusing ducts in their intake system S-duct is also used as inter-turbine diffuser in context of gas turbine design to diffuse the flow between high-pressure and the low-pressure turbine The low-pressure and high-pressure compressors of aircraft gas turbine engines, having centrifugal high-pressure compressor, are connected using S-ducts

LITERATURE SURVEY:

Fox and Kline (1962) investigated the flow regimes of curved diffusers They concluded that flow regimes are dependent on the ratio of centerline radius to throat width, turning angle and area ratio They have also concluded that there was a rapid drop off in allowable area ratio for the first stall limit as the turning angle is increased. The turning angle variation investigated was between 0 to 90 degrees

Bansod and Bradshaw (1972) studied the flow in several S-shaped ducts. They explained the generation of contra-rotating vortices. They showed that the region of low pressure at the exit is due to the vortices carrying free stream flow into the boundary layer.

Kahlil and Weber (1984) analysed the flow inside the curved channel and found that flow structure is strongly controlled by local imbalance between centrifugal force and pressure gradients. The distortion of primary flow was found to be due to migration of low speed flow caused by secondary flow. Also distortion was dependent on Reynaldo number and curvature ratio

Shimizu et al.(1986) studied the performance and internal flow of twisted S-shaped bend diffuser – the so called coiled bend diffuser. They found that the

generates adequate secondary flow inside the diffuser. The relation between diffuser performance and internal flow was studied Some guidelines for designing high performance diffuser are given In their later work Shimizu et al. (1986) described the relationship between bend diffuser characteristics and internal flow in U-shaped and Snake shaped bend diffusers The area ratio, divergent angle and curvature-radius ratios were varied. Also the effects of five different velocity profiles on diffuser performance and internal flow were investigated They conclude that efficiency of these types of diffusers can be considerably increased by selecting the correct inlet velocity distribution and by generating separation-suppressing-type secondary flow inside the diffuser

Sonoda et al (1999) investigated, experimentally and numerically, the flow characteristics within an annular S-duct They studied the effect of two types of inlet boundary layers - thin and thick. The results showed large difference in flow pattern at the exit for the two though the net total pressure loss was nearly same. The aerodynamic sensitivity of S-shaped duct on inlet boundary layer thickness was observed to be very high

Guo and Seddon (1982) investigated the effect of swirl in an S-shaped rectangular duct at different incidences, yaw angle and mass flow ratios The distortion of total pressure at exit was significantly high and a pair of contra-rotating was seen after second bend Guo and Seddon (1982) followed the previous work with investigation of the swirl in an S-duct of typical aircraft intake proportions at different incidences and through flow ratios In order to reduce the magnitude of swirl at high angle of incidence two methods have been studied – one, to change the distortion of the pressure by means of a spoiler and two, to re-energize the separated flow and

swirl at low incidences, which takes classical pattern of two counter-rotating vortices, and a large degree off swirl at high incidence, in the form of single rotating vortex.

Wellborn et al (1992) presented a benchmark aerodynamic data for compressible flow through a representative S-duct. The results show that streamwise flow separation occurs within the duct Details of separated flow region, including the mechanism which drives this complicated flow phenomenon, are discussed The measurements indicate duct curvature induces strong pressure driven secondary flows, evolving into counter-rotating vortices

Majumdar et al examined studied the flow in an S-shaped diffusing duct of rectangular cross-section and having an area ratio of 2. They found that vortical motions developed in the duct change their direction of rotation beyond the inflection plane The overall pressure recovery is low as compared to straight diffuser and a separation pocket was observed at the inflection plane

Johnston (1998) reviewed the diffuser design and performance analysis of simple diffuser with thin inlet boundary layer and subsonic flow using a computational tool, called Unified Integral Method The method provides designer with useful results including pressure recovery, location of separation and stalled regions and exit plane profiles, which may be used to evaluate the total pressure loss and various flow distortion indices. The UIM results were compared with RANS method and other typically used CFD codes and the UIM results were found to be as good, or better then other methods.

Jongen et al (1998) predicted S-duct flow using an incompressible algebraic stress model (that accounts for dissipation rate anisotropies) The composite model is developed for integration to the wall and is calibrated against high Reynolds number,

quantities and turbulence statistics are compared with experimental data and the experimentally observed lag between shear stress vector direction and mean velocity gradient direction is qualitatively predicted

Bushnell and Gad-el-Hak (1991) reviewed the status and outlook of separation control for both steady and unsteady flows They combined both passive and active techniques to prevent or provoke flow detachment

Senoo and Nishi (1974) used conical diffusers with divergence angles 8,12,16,20 and 30 degrees They studied the influence of inlet of inlet boundary layer thickness and location of vortex generators on pressure recovery coefficient They found that vortex generator prevented separation upto divergence angle of 16 degrees and pressure recovery coefficient was approximately equal to that of conventional best conical diffuser

Sullerey and Nagarkoti (1994) investigated the effect of separation control devices namely boundary layer fences and vortex generator on the performance of 2-D curved diffusers The experiments were carried on diffusers having radius of curvature to semi-width ratio 6 and 4 and semi-divergence angles 5 and 6 degrees. The results show substantial improvement in pressure recovery and in quality of flow when compared with those obtained without the use of separation control devices.

Seddon (1984) tested the effect of bottom and sidewall boundary layer fences of various size and combinations in reducing the swirl of an S-duct at high angle of attack It was concluded that large swirl reduction with an improvement of total pressure distribution at high angle of incidences was possible with fences of modest size In some cases the swirl is eliminated or even reversed. At low incidences only a small effect of fences on the mean pressure recovery was observed.

inlet cross-section of a diffusing S-duct At small angle of incidence the spoiler reduced the strength of the counter-rotating vortices observed at the duct exit

Anderson and Gibb (1993) demonstrated that reduced Navier-Stokes RNS3D code can be very effectively used to develop a vortex generator installation to minimize the engine face circumferential distortion by controlling secondary flow This study also established the nature of performance improvements that can be realized with vortex flow control and suggests a set of aerodynamic properties that can be used to arrive at successful vortex generator installation design It indicated that the vortex generator installation should satisfy requirements of minimum engine face distortion along with that of attached flow

Dominey et al (1998) carried out experimental study and computational simulation for an inter-turbine, high curvature S-shaped diffuser. It clearly reveals the generation of significant secondary flows as flow develops through the diffuser The further influence of inlet swirl is also demonstrated

Reichert and Wendt (1993) used a low-profile vortex generator (so-called wishbone types) to improve the total pressure distortions and recovery performance of diffusing S-duct Three parameters, which characterize the vortex generator were systematically varied to determine their effect

1 the vortex generator height,

2 the streamwise location of the vortex generator array and

3 the vortex generator spacing

Each array tested improved the total pressure recovery by reducing the extent of separated flow region The configuration employing largest vortex generator was most effective in reducing distortion but did not produce greatest total pressure

generators with an objective to control the development of secondary flows. They tested 20 configurations of both co- and counter-rotating arrays of tapered fin type vortex generators to reduce total pressure distortion and improve total pressure recovery within an S-shaped diffusing duct The best configuration tested reduced distortion by 50 % while improving the pressure recovery by 0 5% The application of vortex generators here differed from conventional point of view of vortex generators as devices that re-energize the boundary layer by mixing free stream and boundary -layer fluids, rather the objective was to control the development of secondary flows Hingst and Wendt (1994) presented the results of an experimental examination of the vortex structures shed from a low-profile "wishbone" generator The vortex generator height relative to the turbulent boundary layer was varied In all cases a counter-rotating vortex pair was observed

Later, Reichert and Wendt (1996) presented the compilation of previous two studies with additional data on the effectiveness of various vortex generator configurations in reducing exit flow distribution of circular S-ducts. Wendt and Reichert (1996) experimentally studied the effects of an ingested vortex on the flow field of a diffusing S-duct. The ingested vortex is observed to have a strong influence on duct flow field, but only when the vortex trajectory is near the region of separation that exists in the baseline S-duct

Foster et al (1997) conducted measurements in flow through rectangular-to-semiannular transition duct, having area ratio 1 53, to demonstrate the efficacy of vortex generators to reduce the circumferential total pressure distortion

development of an effective design strategy for surface-mounted vortex generator arrays in a subsonic diffuser for transitioning high-speed inlet flow

Scope of Present Work:

The present experimental investigations have the objective of studying the effect of fences and vortex generators in controlling the secondary flow in an S-duct with a uniform inlet flow distortion The parameters considered for assessing the improvement in diffuser performance are

1 Static pressure coefficient (C_p)

2 Distortion coefficient (D_c)

3 Total pressure loss coefficient (ω)

The two S-duct diffusers studied have the same centerline arc length and area ratio thereby keeping the streamwise pressure gradient nearly constant However, as the radius of curvature of centerline arcs is different in the two cases, the diffuser with greater radius of curvature of centerline arcs would be subjected to greater secondary flows In the first diffuser only fences were used while in the second one both fences and vortex generators, separately and in combinations, have been used to assess the improvement in pressure recovery and exit flow distortion The S-duct diffusers under investigation have a rectangular cross-section The results presented do not necessarily represent the optimum performance, but demonstrate large improvements in diffuser performance that are possible with judicious deployment of fences and vortex generators

CHAPTER 2

Experimental Setup

2.1 Description of wind tunnel:

The measurements were carried out in an open-circuit wind tunnel A blower discharged air through a diffuser into a large settling chamber having a honeycomb and three sets of wire mesh screens A contraction section of an area ratio of 17 accelerated the flow into the test section entrance of cross-section area of 380 mm (width) x 305 mm (height) A large contraction ratio ensured a uniform flow at the inlet The free stream turbulence level of the inlet flow was less than 0.5% The diffuser inlet flow was uniform with an average wall boundary layer momentum thickness equal to 0 2% of the inlet width The tests were carried out at a Reynolds no of 7 8x10^5 based on the diffuser inlet width

2.2 Experimental test section:

S-duct diffuser. The S-duct diffusers under investigation have rectangular cross-section of aspect ratio 0 8 at the inlet and an inlet cross-section of 380 mm x 305 mm The area ratio for both the diffusers was 1.35 The diffuser geometries are shown in Fig 1 and Fig 2 The two diffusers have been designed to experience different curvature effects However as the area ratio and the centerline arc lengths are same in the two cases, the streamwise pressure gradient would be similar. The curvature arc length, of the two the diffusers, is equal to the length of a 6-degree semi-divergence angle equivalent straight diffuser of same area ratio. The test diffuser was designed with linear increase in area distributed normal to the centerline. The test duct

shape was obtained by joining points obtained on both the sides of the centerline arc on the basis of linear increase in area The top and bottom duct walls were made of plywood (10mm thick) and the curved sidewalls were of Perspex sheets (3mm thick) The top and bottom walls were parallel. For the first diffuser (Fig. 1), the centerline radius of curvature to half width ratio was 6 and for the second diffuser (Fig. 2) it was 4, which are consistent with the typical aircraft intake values. Two planar circular arcs with identical radii defined the duct centerline However, as the arc radius was different in two cases, the two diffusing ducts subtended different angles (16 and 24 degrees respectively)

Between the contraction and the S-duct, a straight duct of 300 mm length was provided to obtain fully developed, zero pressure gradient turbulent boundary layer at the diffuser inlet A constant area duct extension of 300 mm length was also placed at the diffuser exit to provide smooth, continuos flow exiting the duct

Several wall pressure tapings (0.8 mm diameter) were provided at different planes along both the curved surfaces and along top wall centerline to measure wall static pressure For wall shear stress measurements Preston tubes (0 8 mm diameter) were used on the inner and the outer walls of the diffuser. The detailed geometry of the test ducts along with measuring stations is shown in Fig. 1.

Fences and Vortex Generator. The different fence configurations with which S-duct diffuser flow measurements have been taken are shown in Fig. 1 The fences were made of 3 mm thick Aluminium sheet. The edges of the fences were rounded off Based on initial observations, involving measurements using fences of different heights in only the first bend of S-duct diffuser (R/r=6), the fence height was kept uniform at 120% of measured boundary layer thickness (without any fences) at the inflection plane The fences were inserted through slots along the top and bottom wall

centerlines The fences were also tried on inner and outer walls. The results indicated an increase in the losses and a drop in static pressure rise and hence were dropped from subsequent measurements. Different fence configurations were obtained by varying the height and position of the fences in the first and the second bend. Four different fence configurations used are B, C, D, and E. The configuration A is the diffuser without any wall mounted fences The best fence configuration, i.e. E, obtained from the tests on the first diffuser (R/=6) was tried in the second diffuser (R/r=4) The fence height was varied to obtain the optimum height for this diffuser

The vortex generator design is shown in Fig 2 alongside the diffuser geometry The geometry chosen was similar to the one given by Wendt and Hingst (1994) The height of the vortex generator was however greater and about 60% of the boundary layer thickness (of the bare duct) at the point where the vortex generator (tip) was fitted The base of the vortex generator was curved in accordance with the wall profile. The locations of the vortex generators were selected on the basis of wall pressure distribution The most appropriate location considered was just prior to the region of high adverse pressure gradient At each location, a pair of vortex generators was used The measurements were carried out with vortex generators on both the walls, with vortex generators only on a single wall and using fences only Also, fences and vortex generators were tried simultaneously to observe the combined effect of the two.

2.3 Instrumentation and measuring techniques:

Measurements include diffuser wall static pressure distributions, mean velocities, boundary layer and skin friction measurements and flow angularity measurements A Furness (FC012 model) digital multi-channel micro-manometer was used for all pressure measurements.

The inlet velocity distribution was obtained using the pitot tube. The static pressure measurements were taken with wall pressure tapping at eight stations on each diffuser The last station was at some distance from the diffuser exit on the straight duct attached at the diffuser exit Each station had nine pressure taps of 0 8 mm diameter There were four additional pressure taps at the inflection plane For all measurements the inlet static pressure was taken as the reference pressure. The static pressure recovery coefficient is defined as

$$C_P = (p-p_{ref}) / (1/2\ \rho V^2_\infty) \quad (1)$$

Where, p is the wall static pressure and p_{ref}, is the diffuser entry static pressure The C_P values are expected to be within one-percent accuracy

The boundary layer measurements were made on all four walls at inlet, inflection and the exit planes of the S-duct diffuser A 0 8 mm diameter pitot probe was used for this purpose

The total pressure and velocity measurements were made using a five-hole conical probe of diameter 6 4 mm The probe also provided the values of local static pressure and flow angularity For probe traverse, an accurate three-dimensional traverse system (least count 0 5 mm) was used Detailed flow measurements using five-hole probe, aligned perpendicular to the radial direction, were made at the inflection and the diffuser exit plane for different fence and vortex generator configurations tested. The total pressure measurements are expected to be within one percent accuracy and the flow angles are expected to be accurate within one degree

The wall skin friction measurements were made using wall mounted Preston tubes of 0 8 mm diameter. These tubes were fitted along the centerline of inner and outer walls at seven stations The skin friction measurements are expected to be within 2% accuracy. It is based on the assumption of a universal inner law (or the law

of wall, $U/U_\tau = f(U_\tau y / U)$, common to boundary layers and fully developed flows. The coefficient of friction was calculated according to the formula

$$C_f = \tau_w / (0.5\rho V^2) \quad (2)$$

Where, τ_w is shear stress τ_w is obtained from the formula

$$\tau_w d^2 / (4\rho\upsilon^2) = F(\Delta p_p d^2 / 4\rho\upsilon^2) \quad (3)$$

where, Δp_p is the Preston tube reading, d is Preston tube diameter, υ is the kinematic viscosity of the fluid Patel (1964) showed that the function F can be readily determined from the measurements in fully developed pipe flow

2.4. Five Hole Pressure Probe:

A five-hole conical pressure probe (shown in Fig. 3a) was fabricated as per the design given by Ohman and Nguyen (1993) and was calibrated following the procedure same as that followed by Poddar and Sharma (1998) The mechanism designed for holding the probe during calibration, the calibrator, is shown in Fig 3b

The incompressible flow can be divided into two flow regimes: inner sector and outer sector flow The flow remains attached for flow angularities nearly equal to half cone angle of the probe (flow angle upto 30 degrees for the probe used here) and is named inner sector flow Only this regime was of interest to us as flow angles greater then this are not expected in the S-duct diffuser tested and hence the probe was calibrated for this region only The probe provided the values of local total pressure (with respect to the reference pressure used), local static pressure, flow velocities (all the three components) and the flow angularity. The inlet static pressure was used as the reference pressure for all the probe measurements and hence the various pressure readings obtained are with reference to the inlet static pressure. The non-dimensional parameters used to obtain various values are defined as follows.

$$C_\alpha = (P_5 - P_3) / (P_1 - P_{av}) \quad (4a)$$

$$C_\beta = (P_2 - P_4) / (P_1 - P_{av}) \quad (4b)$$

$$C_q = (P_1 - P_{av}) / (P_{ol} - P_\infty) \quad (4c)$$

$$C_o = (P_1 - P_{ol}) / (P_1 - P_{av}) \quad (4d)$$

The calibration of 5-hole probe involves measuring the P_i's under known flow conditions i e P_{ol}, $q_{\infty l}$, α (pitch angle) and β(yaw angle) The above defined parameters are calculated and plotted with respect to α and β

In actual application of the probe, the local flow properties at the probe tip are determined by measuring all the five port (holes) pressures (P_i's)

CHAPTER 3

Results and Discussions

The first set of tests was carried out on bare S-ducts diffusers. The boundary layer measurements at the inflection plane and the duct exit did not indicate any flow separation in either case These measurements along with the wall static pressure distribution provided an idea of boundary layer thickness and the nature of adverse pressure gradients in the diffusers The selection of particular fence configurations and the location of vortex generators were based on these measurements

The first S-duct diffuser (R/r=6) expectedly had much less steep pressure gradient as compared to the more curved second diffuser (R/r=4). Therefore, it was considered appropriate to use vortex generators only for the second diffuser, which showed more likelihood of flow separation Presented below are the results of the two diffusers of radius ratio 6 and 4 in that order

Diffuser 1(R/r=6). The C_p distribution on the inner and outer walls for the first diffuser is shown in Fig 4 for all five cases with and without fences. It can be observed that the pressure recovery improves significantly both on the inner and outer walls especially with fence configurations D and E The inner and outer wall pressures at a particular station can be seen to differ considerably leading to secondary flows The fences are expected to reduce secondary motion and this is confirmed by these results It is seen that there is no significant adverse pressure gradient on either wall and particularly on the inner wall The probability of flow separating is very less and that is why the vortex generators were not used in the case of this diffuser On the inner wall, initially there is a rise in pressure, then a drop and

again an increase some degrees after the inflection plane This is so because the flow accelerates on the inside of the bend and decelerates on the outside. On the outer wall continuos rise in static pressure is seen

The diffuser centerline pressure distribution (in a way indicative of average pressure recovery) is shown in Fig 5 The role of fences in increasing the pressure recovery is quite evident from this figure All the configurations of fences tried yielded an improvement in the static pressure recovery.

On the basis of average static pressure at the exit of the duct, 18.6% improvement in the C_p value was obtained for the configuration E as compared with the bare duct

From the Preston tube measurements no flow separation was observed on either walls, with or without fences The distribution of skin friction coefficient along the inner and outer wall is shown in Fig 6 The values towards the exit are comparable with those given by Johnston (1998) for straight and conical diffusers (unstalled) of 5-degree semi-divergence angles The skin friction coefficient values obtained with the fences were more then those obtained for the bare duct. This indicates a reduction in the tendency of flow to separate when the fences are employed

The exit momentum thickness for the bare diffuser (as percentage of inlet width) is 2.16% on outer wall and 0.96% on the inner wall. For diffuser with fences (configuration B) the corresponding values are 1.86% and 0 44%. The reduced momentum thickness is indicative of lower losses when the fences are employed.

The total pressure losses are expressed in terms of total pressure loss coefficient ω, defined as

$$\omega = (p_{o2av} - p_{o1}) / (1/2\rho V^2) \qquad (5)$$

Fig 7 presents the loss coefficient (ω) distribution at the exit of the S-duct diffuser for the bare duct and the best configuration tested (i e E). The exit total pressure loss coefficient is 0 16 for the bare diffuser and 0 10 for the diffuser with configuration (E) The expected accuracy of loss coefficient values is within two percent

The total pressure non-uniformity is measured in terms of distortion coefficient, D_C, defined as below

$$D_C = (p_{oav} - p_{omin}) / q_{av2} \quad (6)$$

The D_c values for the two cases are 0 662 and 0 588 respectively indicating improvement in flow uniformity with fences indicating improvement in flow uniformity with fences

Fig 8 presents the velocity distributions at the exit plane of the bare S-duct diffuser and the diffuser with fence configuration E An improvement in the outflow quality can be clearly observed by comparing figures 8(b) and 8(c)

Fig 9 and Fig 10 show the transverse velocity distributions, in terms of non-dimensional velocity parameter defined as the ratio of local cross flow velocity to the maximum cross flow velocity in that plane, at the inflection and the exit planes respectively Considering Fig 9 it may be seen that at inflection plane the direction of most of the cross flow velocities are towards the inner wall because of the inertia of the flow Fig 10(a) clearly reveals two counter-rotating vortices at the diffuser exit. The secondary flow reduction with fences can be observed by comparing Fig. 10(a) and Fig 10(b). The cross velocity vectors in the Fig. 10(b) do not show any distinguishable vortical motion. An overall reduction in secondary flow was observed The maximum value of the transverse velocity in the bare duct was about 17.5% of the streamwise velocity while with the fences this reduced to about 14.8%

For obtaining the optimum fence height, which came out to be 120% of boundary layer thickness at the inflection plane, fences of different heights were used only on the bottom wall of the first bend Later these results were confirmed by tests with configuration E

Diffuser 2 (R/r=4). This diffuser had higher curvature as compared to the previous one and hence greater secondary flows were expected in it Initially after measurements on the bare duct, measurements were carried out with fence configuration E for different fence heights For the case of 15 mm fence height, the height was less then the boundary layer thickness at the inflection plane Further measurements were carried out using vortex generators alone and in combination with fences

Fig 11 presents the inner and outer wall C_p distribution with and without fences The trend was same as that observed in the previous diffuser but a steep adverse pressure gradient was observed on the inner wall a little after the inflection plane. On comparing the pressure distribution for the present diffuser with that of the first diffuser (Fig 4), it can be noticed that at any station the pressure difference between inner and outer walls is much more for the second diffuser. Secondary flows in curved ducts arise due to this pressure difference and hence diffuser 2 would be experiencing greater cross-flows and consequently more losses.

Fig. 12 shows the duct centerline C_p distribution, which is best for the configuration having fence height of 50 mm. With vortex generators fitted on the inner and outer walls some of the static pressure taps were covered and hence C_p distribution for the diffuser fitted with vortex generator is not shown.

In Fig 13, skin friction measurements on the bare S-duct are shown The inner wall C_f approaches zero near the diffuser exit Comparing with diffuser 1, C_f values

on the C_f distributions, it was considered that vortex generators would be more effective in the diffuser 2 and hence were used only for this diffuser

For the bare diffuser, momentum thickness (as percentage of inlet width) is 2 53% on the outer and 1 2% on the inner wall For the diffuser with fences of height 50 mm the two values are 2 01% and 0 62% respectively

The streamwise velocity distribution at the inflection plane for the bare duct is shown in Fig 14 and at the diffuser exit plane for the four different configurations tested is shown in Fig 15 The figures reveal a reduction in exit flow distortion with various fences and vortex generator configurations

The loss coefficient (ω) distribution at the inflection plane is shown in Fig 16 Fig 17 presents the loss coefficient distributions at the diffuser exit for the four configurations tested The complete results including static pressure rise, loss coefficient and distortion coefficient rise are given in Table 1.

Table 1

Exit property	Bare duct	With fences	With VG	With VG and fences
C_p	0 267	0 3	0 269	0.298
ω	0 17	0.121	0.142	0.147
D_c	0 786	0 707	0.591	0 744

*VG - Vortex generators

The vortex generators alone do not lead to much improvement in C_p The maximum C_P value was obtained with diffuser having fences only This value was 12 3% more compared to that of the bare duct Comparatively the improvement in static pressure is significantly more with fences. However minimum distortion coefficient was obtained with vortex generators A reason for these results seems to be that the improvement in

height was not varied and it was kept within the boundary layer the effect was less as compared to that with fences Moreover it is likely that the vortex generators created more losses as compared to the fences, which were very thin. The reduction in flow distortion and total pressure losses obtained with a combination of vortex generator and fences is comparatively less

The transverse velocity distributions at the inflection and the exit plane are shown in Fig 17 and Fig 18 respectively At the exit plane, the maximum value of the cross-flow velocity for the bare duct was 25% of the freestream velocity This value reduced to 20.8% with the fences The results show a reduction in cross flow velocities with the use of fences

Fig 19 compares the centerline pressure distribution for the two diffusers without any fences or vortex generators and their best configurations with the fences. There is significantly greater pressure recovery for the first diffuser when compared with the second diffuser This shows the effect of the centerline curvature on the diffuser performance The rise in static pressure recovery with the use of fences can be seen

Fig 20 shows the static pressure distribution across the top wall at the diffuser exit for all the fence and vortex generator configurations tried It is quite evident from this figure that a considerable improvement in static pressure rise is obtained with the use of fences on both top and bottom walls

CHAPTER 4

Conclusion

In diffuser 1 (R/r=6) the use of fences significantly improved the diffuser performance for all the fence configurations tested The best configuration, E, having fences along both top and bottom wall centerlines, gave an increase of 18 6 percent in the static pressure recovery, decreased the total pressure loss coefficient from 0 16 to 0 10 and decreased the flow distortion coefficient at the duct exit from 0 662 to 0 588. Among the different fence heights used the fence height equal to 120 percent of boundary layer thickness at the inflection plane resulted in best diffuser performance The improvement in the diffuser performance was obtained due to reduction in the secondary flows brought about by the fences In diffuser 2 also, the maximum improvement in static pressure recovery was obtained with the configuration employing fences only but here the fence height required, for this improvement, was greater compared to the previous diffuser An improvement of 12 5 percent in Cp value at the diffuser exit was obtained with this configuration The total pressure loss coefficient decreased from 0.17 to 0 12 and the distortion coefficient decreased from 0 786 to 0 707 It was observed that the fence height giving the best performance would vary depending upon the centerline curvature

In the second diffuser fences as well as vortex generators were employed in view of steeper adverse pressure gradient as compared to the first diffuser. The vortex generators alone gave little improvement in static pressure as compared to the fences, however there was a reduction in flow distortion A reason for these results seems to be that the improvement in both the cases arises due to reduction in secondary flows. However the vortex generators created their own losses, the fences being very thin generated very less losses. All the vortex generator configurations tested did show

some improvement in total pressure recovery, static pressure rise and flow quality The combination of fences and vortex generators proved comparatively less effective in reducing he exit flow distortion and total pressure recovery

With the application of fences, the maximum value of the cross flow velocity decreased from 17 5 percent to 14 8 percent of the axial velocity in first diffuser and from 25 percent to 20 8 percent of the axial velocity in the second diffuser

The fences were used only on the top and bottom wall centerlines So it cannot be necessarily concluded that the configuration giving the best performance is the optimum arrangement of fences However, it is likely that the optimum performance can be obtained by increasing the number of fences and their height, depending upon the centerline curvature

REFERENCES

Anderson, B H , and Gibb, J , 1993, "Study on Vortex Generator Flow Control for the Management of Inlet Distortion," Journal of Propulsion and Power, Vol 9, No 3, pp 422-430

Bansod, P , and Bradshaw, P , 1970, "The flow in S-shaped ducts," Aeronautical Quarterly, Vol 23, pp 141-140

Dominy, R G , Kirkham, D A , and Smith, A D , 1998, "Flow Development Through Interturbine Diffusers," Journal of Turbomachinery, Vol 120, pp 298-304

Foster, J , Wendt, B J , Reichert, B A , and Okiishi, T H, 1997, "Fow Through a Rectangular-to-Semiannular Diffusing Transition Duct," Journal of Propulsion and Power, Vol 13, No 2, pp 312-317 Guo, R W , and Seddon, J , 1983, " The swirl in S-duct of typical air intake proportions," Aeronautical Quarterly, pp 99-129

Guo, R W , and Seddon, J , 1983, "Swirl characteristics of an S-duct air intake with both horizontal and vertical offsets," Aeronautical Quarterly, pp 130-146

Guo, R W and Weng, P F , 1994, "New method of Swirl Control in a Diffusing S-duct," AIAA Journal, Vol 30, No 7. Technical Notes, pp 1918-1919

Gad-el-Hak, M , and Bushnell, D M , 1991, "Separation control Review," Journal of Fluids Engineering, Vol 113, pp 5-29

Hingst, W R , And Wendt, B J , 1994, "Flow structure in the Wake of a wishbone vortex generator," AIAA Journal, Vol 32, No 11, Nov , pp 2234-2240

Johnston, J l , 1998, "Review Diffuser Design and Performance Analysis by a Unified Integral method," Journal of Fluids Engineering, Vol 120, pp.6-18

Jongen, T , Mompean, G , and Gatski, T B , 1998, "Predicting S-Duct Flow Using Composite Stress Model," AIAA Journal, Vol 36, No 3, pp 327-335

Majumdar, B , Singh, S N , and Agrawal, D P , 1997, " Flow Characteristics in S-Shaped Diffusing Duct," International Journal of Turbo and Jet Engines, Vol 14, pp 45-57

Majumdar, B , Mohan, R., Singh, S.N , and Agrawal, D.P., 1998, " Experimental Study of Flow in High Aspect Ratio Curved Diffuser," Journal of Fluids Engineering, Vol 120, pp. 83-89.

Ohman, L.H., and Nguyen, V.D, 1993, "Applications of the Five-hole Probe Technique For Flow Field Surveys at the Institute for Aerospace Research," AGARD Meeting on ' wall Interference, Support Interference and Flow Field Measurements', October 1993.Patel, V.C., 1965, "Calibration of Preston Tube and Limitations on its use in Pressure Gradients," Journal of Fluid Mechanics, Vol. 23, pp. 812-208.

Poddar, K., and Sharma, G., 1998, "Manufacture, Calibration and Application of 7-Hole Pressure Probe," Report No. AE/NWTF/INSTR/98/02, I.I.T. Kanpur.

Reichert, B.A., and Wendt, B.J., 1993, " An Experimental Investigation of S-Duct flow Control Using arrays of Low Profile Vortex Generator," AIAA Paper 93-0018.

Reichert, B.A., and Wendt, B.J., 1994, " Improving Diffusing S-Duct Performance by Secondary Flow Control," NASA Technical Memorandum 106492.

Reichert, B.A., and Wendt, B.J., 1996, " Improving Curved Subsonic Diffuser with Vortex Generators," AIAA Journal, Vol. 34, No. 1, pp.65-72.

Seddon, J., 1984, " Understanding and countering the swirl in S-ducts: tests on the sensitivity of swirl to fences," Aeronautical Journal, pp. 130-146.

Senoo, Y., and Nishi, M., 1974, "Improvement of the Performance of the Central Diffuser by Vortex Generators," Journal of Fluids Engineering, vol. 96, pp. 4-10.

Shimizu, Y. Nagafusa, M., Sugino, K., and Kubota, T., 1986, "Studies on performance and internal fl(w of twisted S-shaped bend diffuser- the so-called coiled bend diffuser: 1st Report," Journal of Fluids Engineering, Vol. 108, pp. 289-296.

Shimizu, Y. Nagafusa, M., Sugino, K., and Kubota, T., 1986, "Studies on performance and internal flow of U-shaped and Snake shaped bend diffuser: 1st Report," Journal of Fluids Engineering, Vol. 108, pp. 297-303.

Sonoda, T., Arima, T., and Oana, N., 1999, "The Effect of Inlet Boundary Layer Thickness on the Flow Within an Annular S-Shaped Duct," Journal of Turbomachinery, Vol. 121, pp. 626-634.

Sullerey, R.K., and Nagarkoti, A.K.S., 1994, "Effect of separation control devices on the performance of curved diffusers",*

Wendt, B.J, and Dudek, J.C., 1998, "Development of Vortex Generator Use for a Transitioning High-Speed Inlet," Journal of Aircraft, Vol. 35, pp. 536-543.

Wendt, B.J., Greber, I., and Hingst, W.R., 1994, "Structure and Development of Streamwise Vortex Arrays Embedded in a Turbulent Boundary Layer," AIAA Journal, Vol. 31, No. 2, pp. 319-325.

Wellborn, S.R., Reichert, B.A., and Okiishi, T.H., 1992, "An Experimental Investigation of the Flow in a Diffusing S-Duct," AIAA Paper 92-3622.

Wendt, B.J. nd Reichert, B.A., 1996, " Vortex Ingestion in a Diffusing S-Duct Inlet," Journal of Aircraft, Vol. 33, No. 1, Jan.-Feb.

Yaras, M.I., 1996, "Effects of Inlet Conditions on the Flow in a Fishtail Curved Diffuser With Strong Curvature," Journal of Fluids Engineering, Vol. 118, pp.772-778.

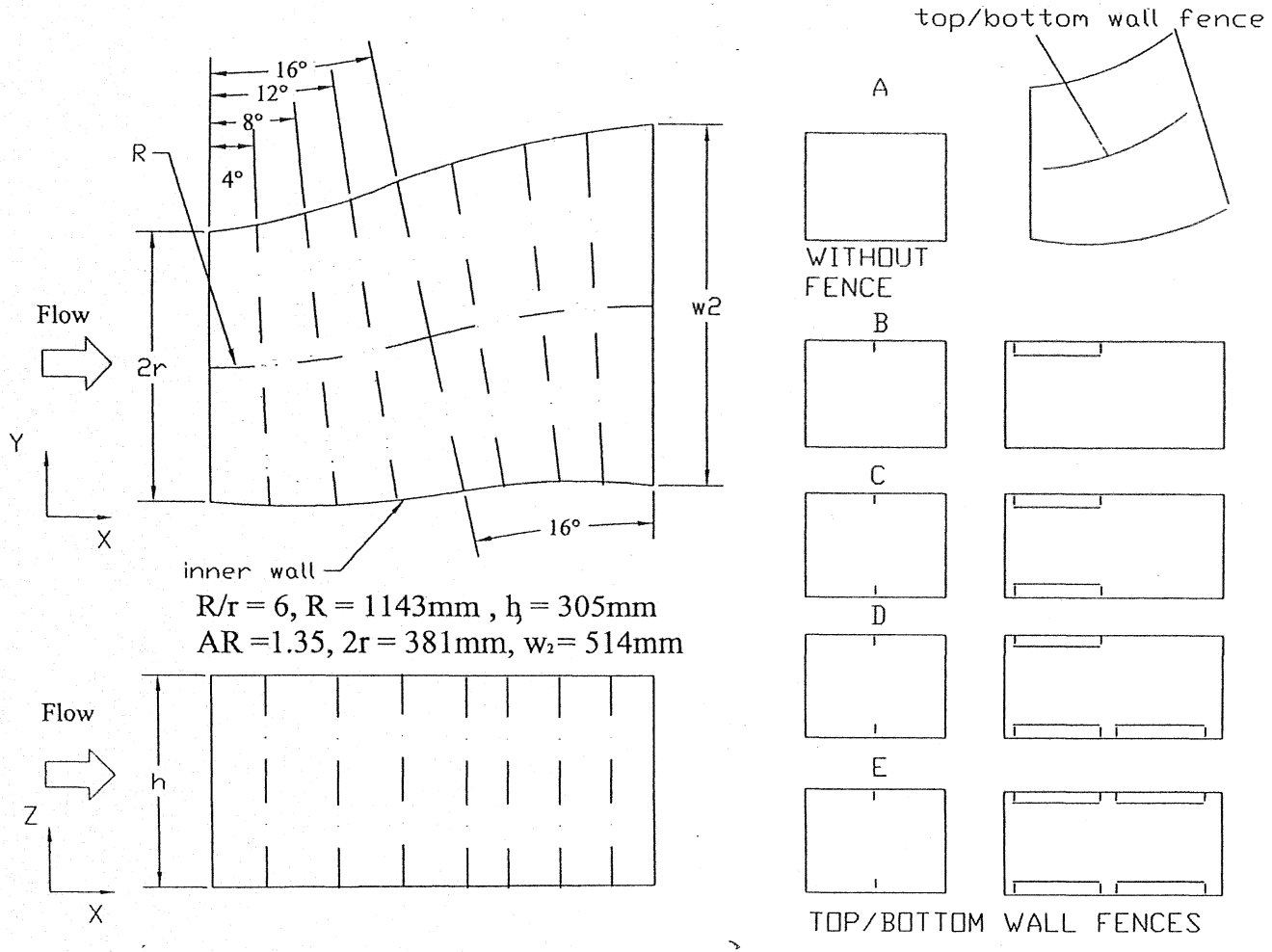

Fig. 1 Layout of S-duct diffuser and fence configurations

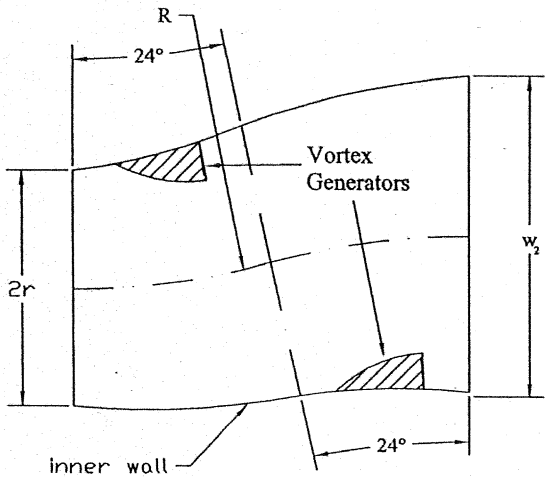

R/r = 4, R =762mm, 2r =381mm
AR=1,35, h=305mm, w2=514.5mm

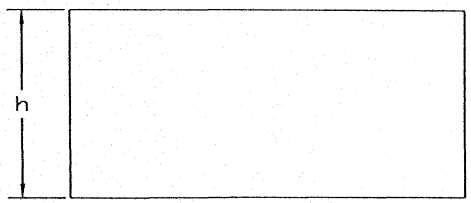

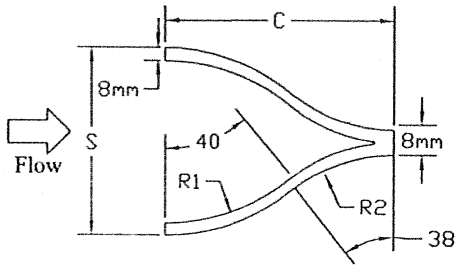

	Outer Wall	Inner Wall
R1	126	110
R2	104	91
R3	243	213
h	40	35
s	109	95
c	147	129
R4	Outer Wall Radius	Inner Wall Radius

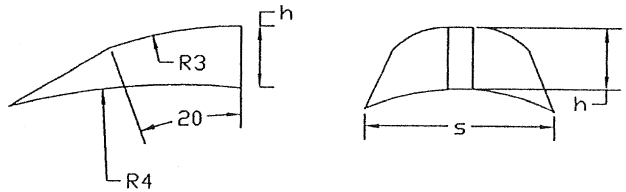

Vortex generator geometry

Fig. 2 Diffuser geometry with vortex generator

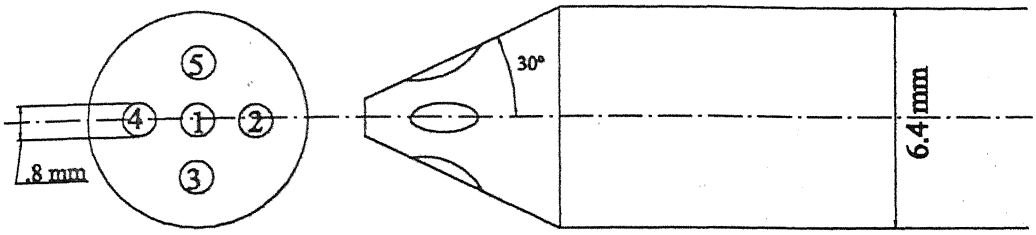

(a) Five Hole Probe

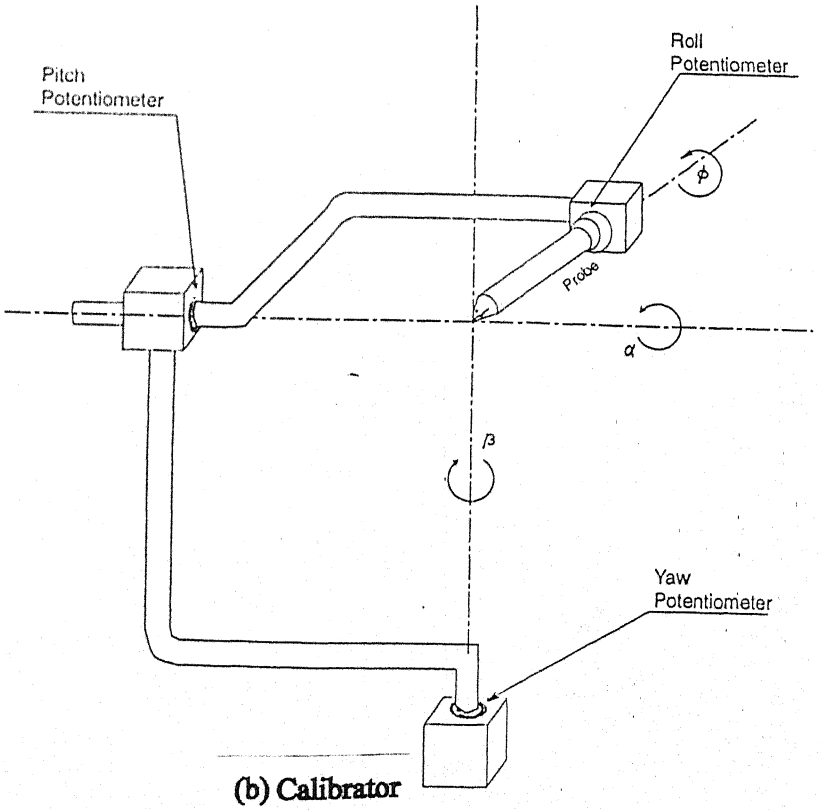

(b) Calibrator

Fig. 3 Probe geometry and Calibrator

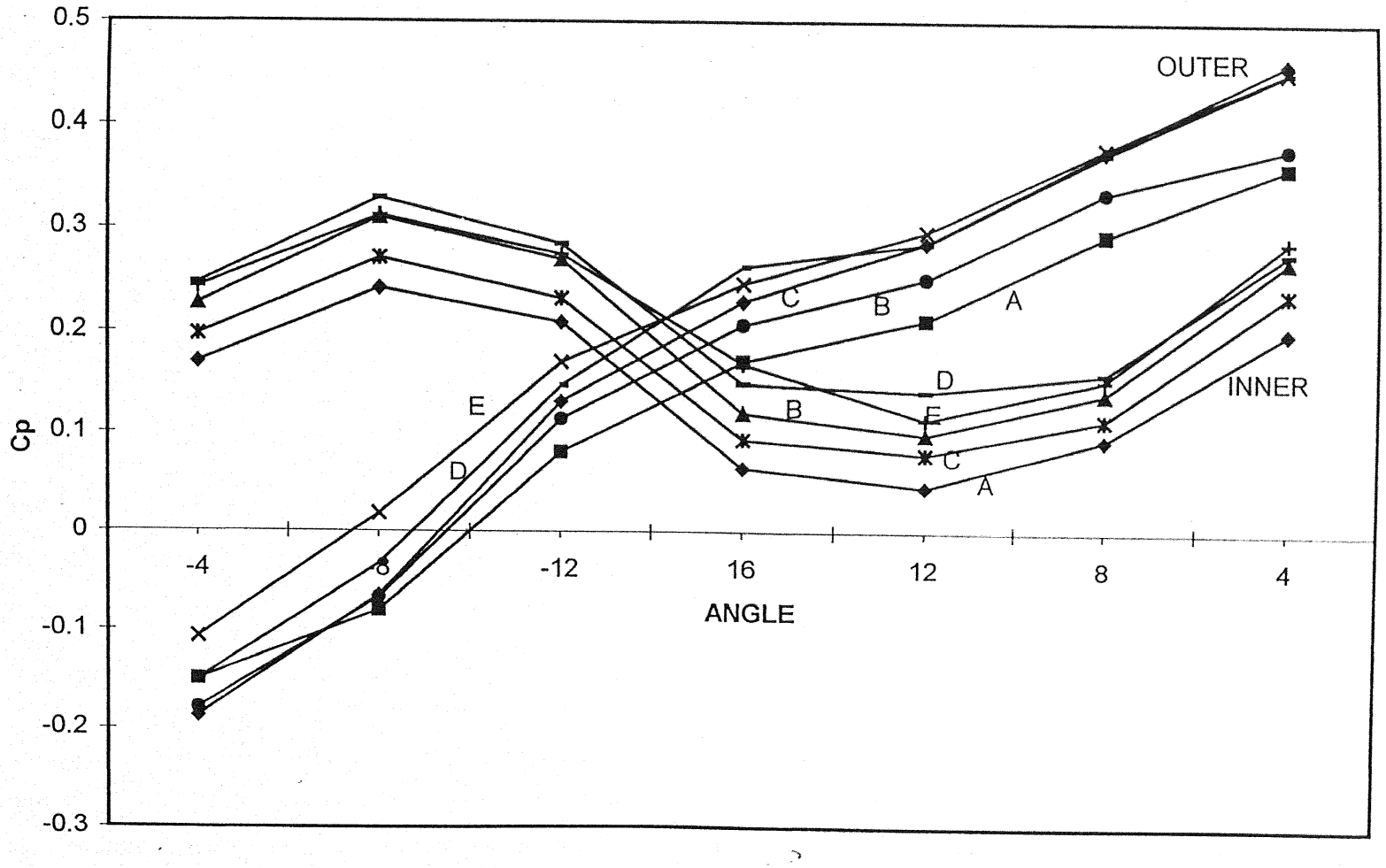

Fig. 4 Cp distribution in diffuser1 (R/r=6) for different fence configurations

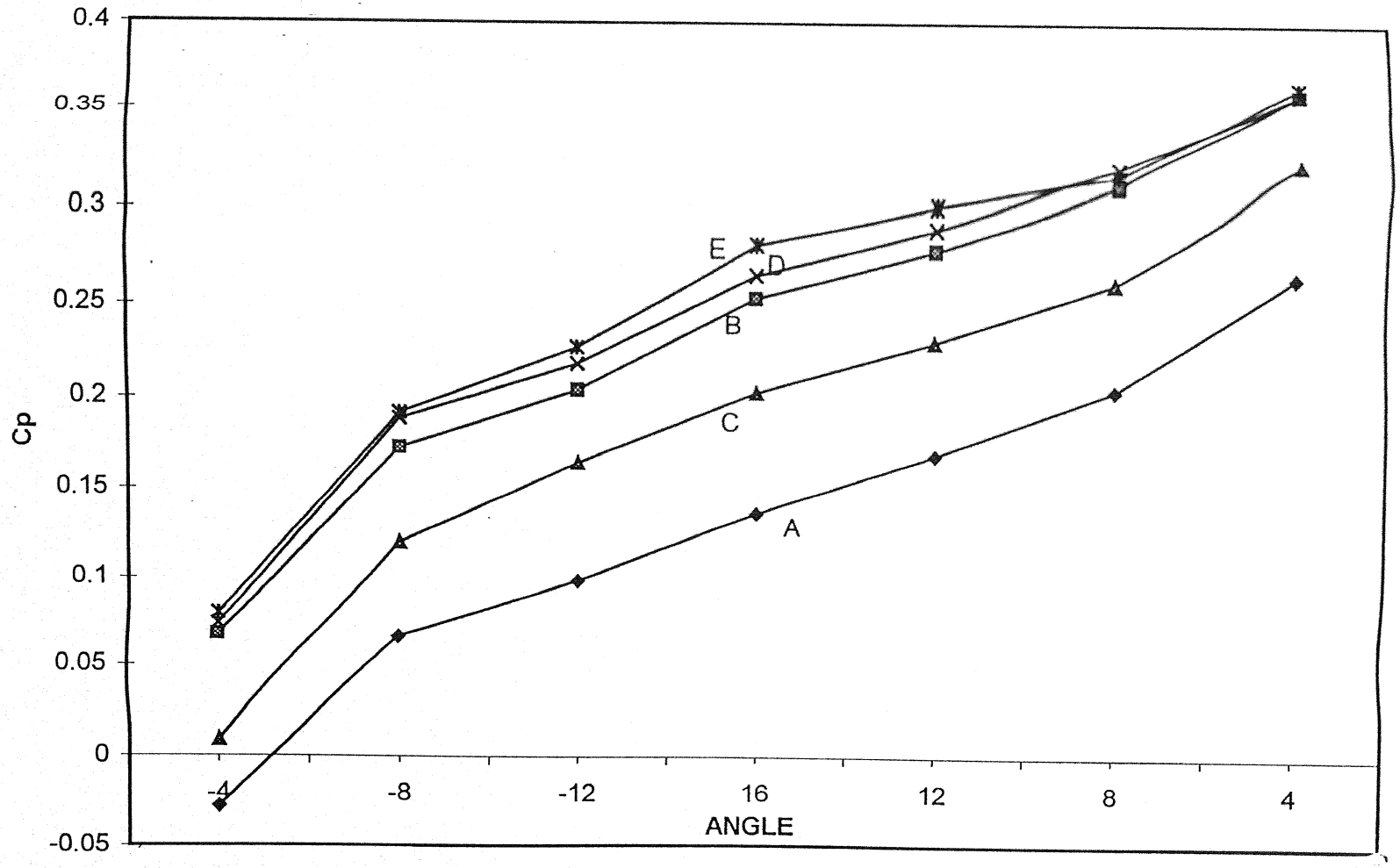

Fig.5 Centerline Cp Distribution for Different Fence Configurations

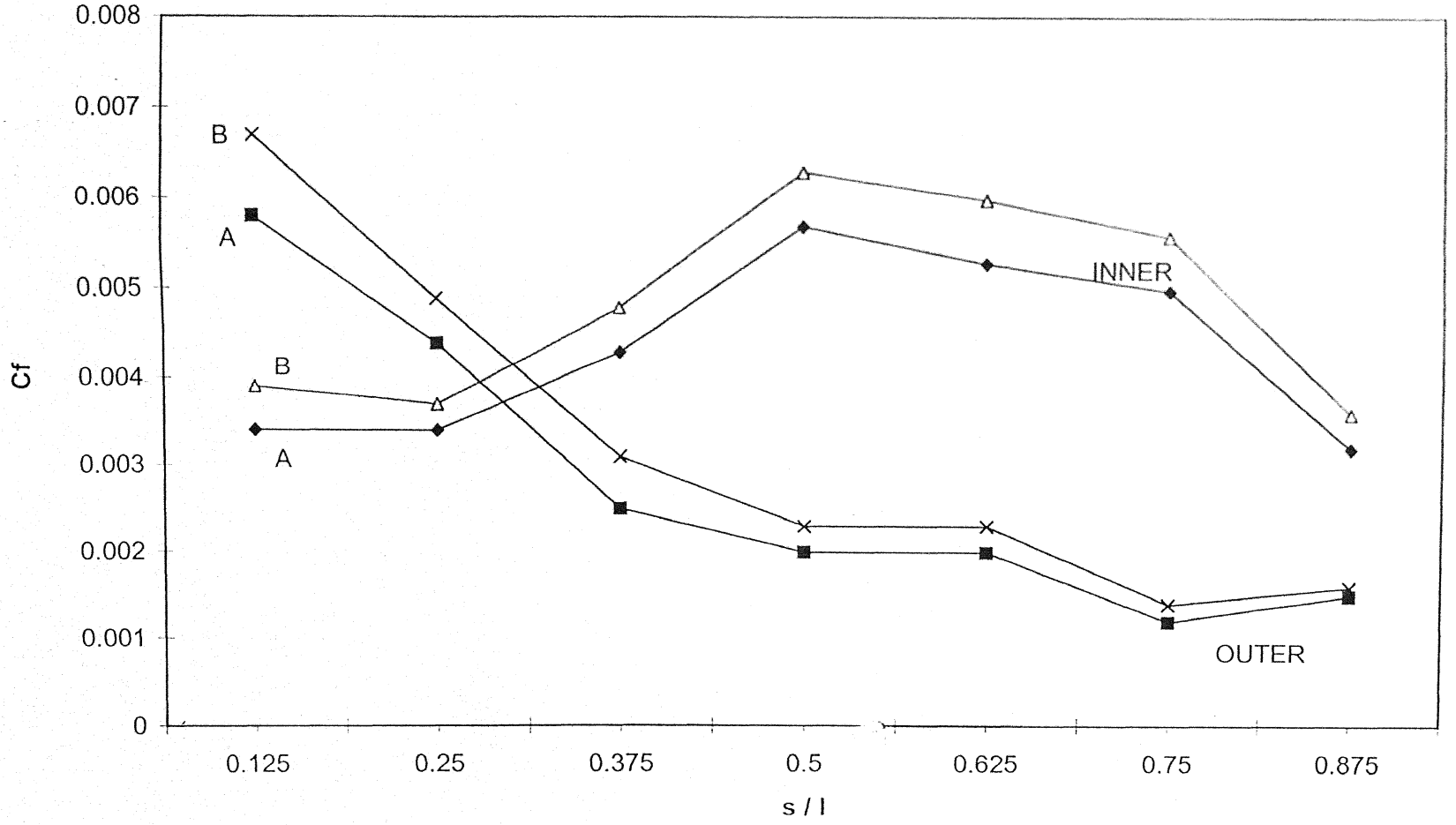

Fig. 6 Variation of skin friction coefficient along the side walls

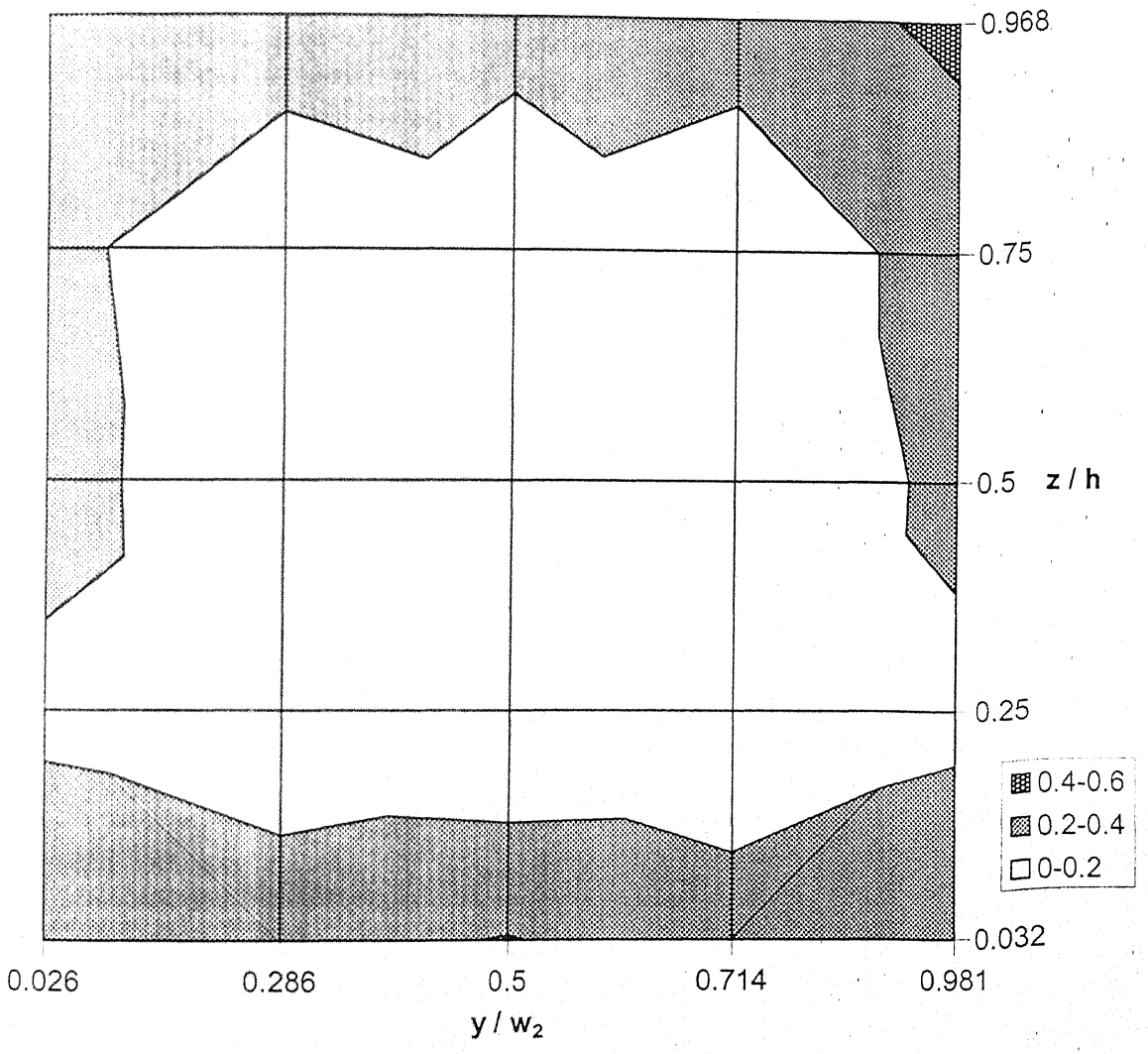

Fig. 7(a) Loss coefficient distribution at diffuser1(R/r=6) exit

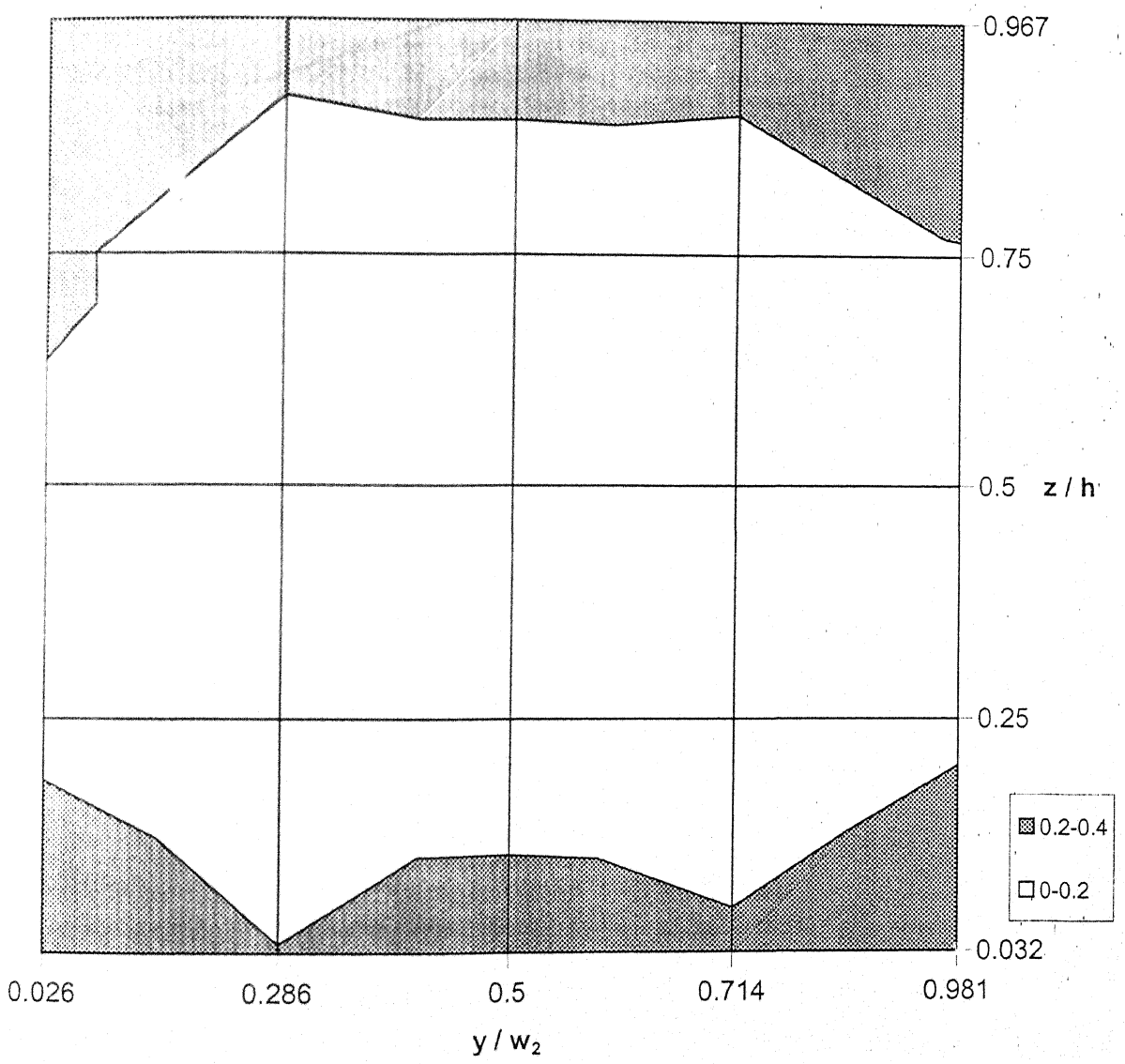

Fig. 7(b) Loss corfficient distribution for diffuser1(R/r=6) with fences

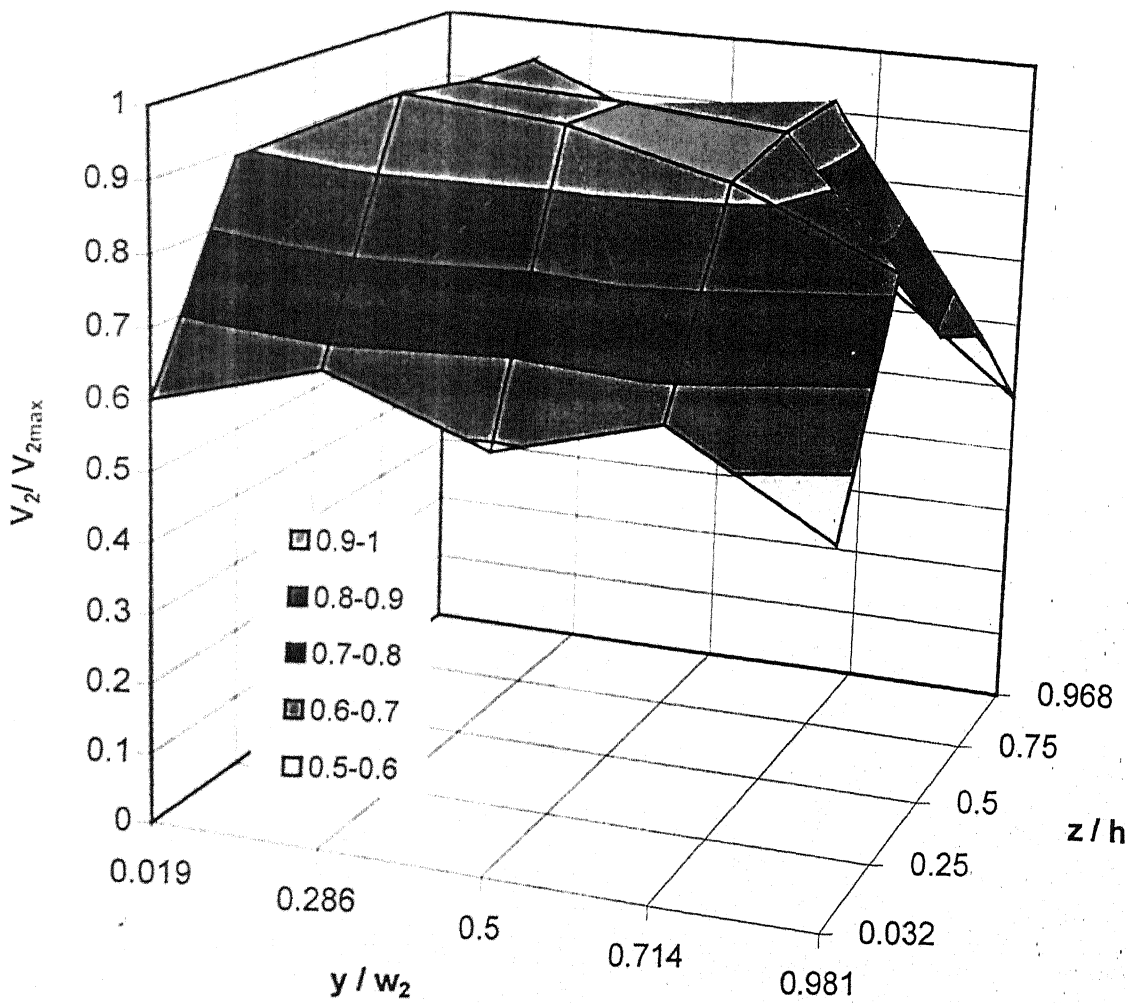

Fig. 8(a) Velocity distribution at diffuser (R/r=6) exit

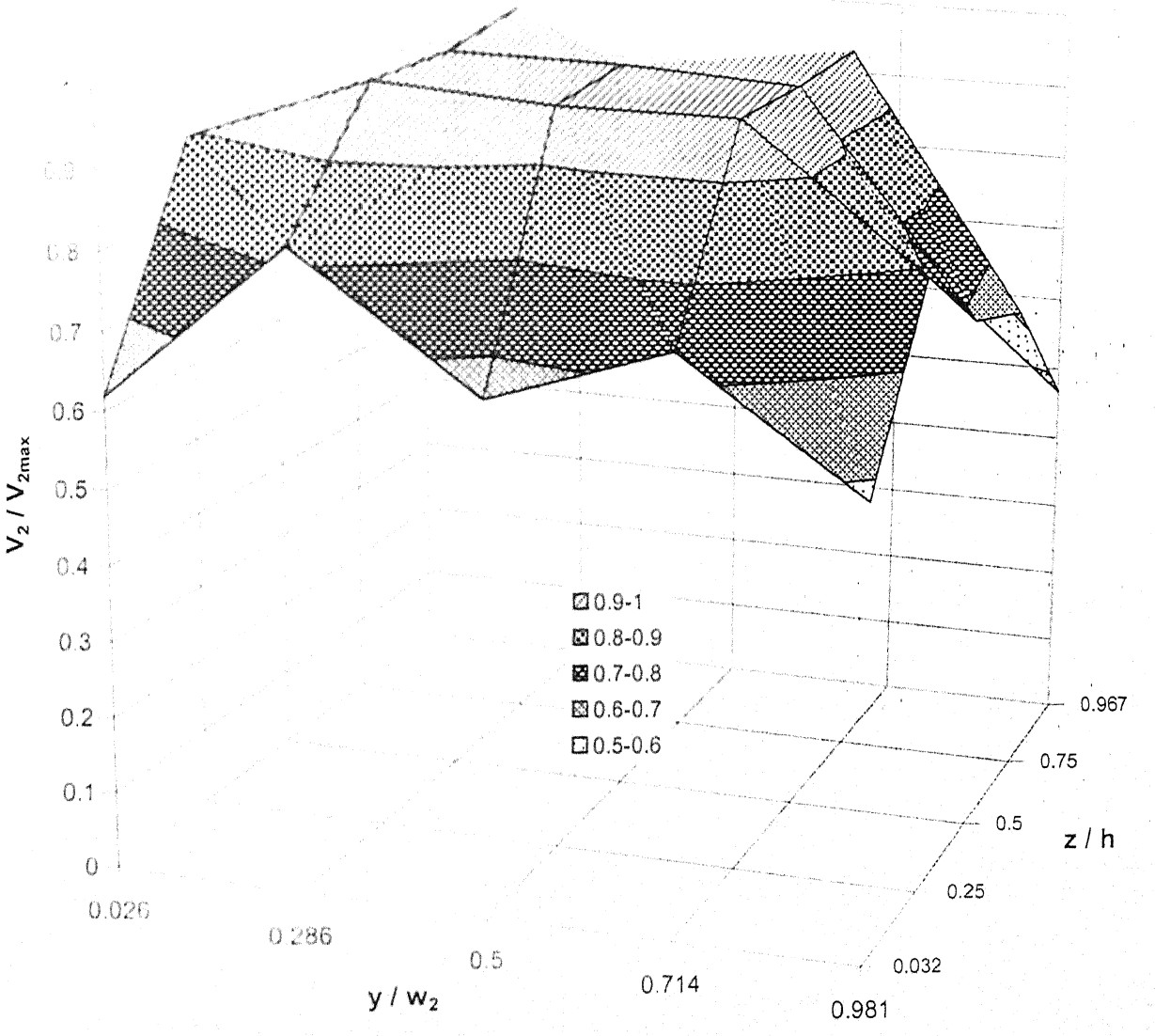

Fig. 8(b) Velocity distribution at diffuser1(R/r=6) exit with fences

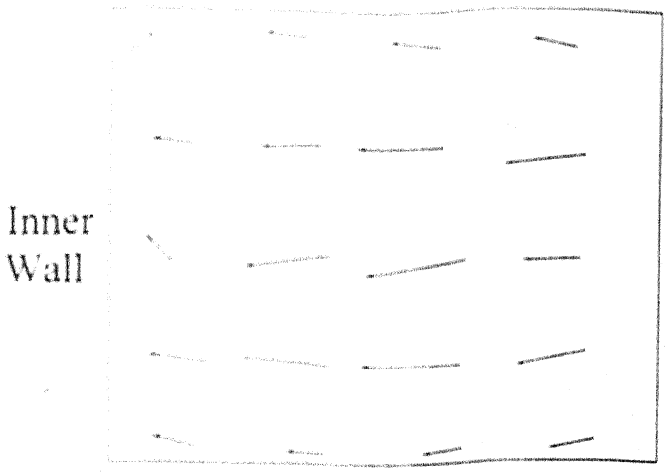

Fig. 9 Transverse velocity distribution at inflection plane

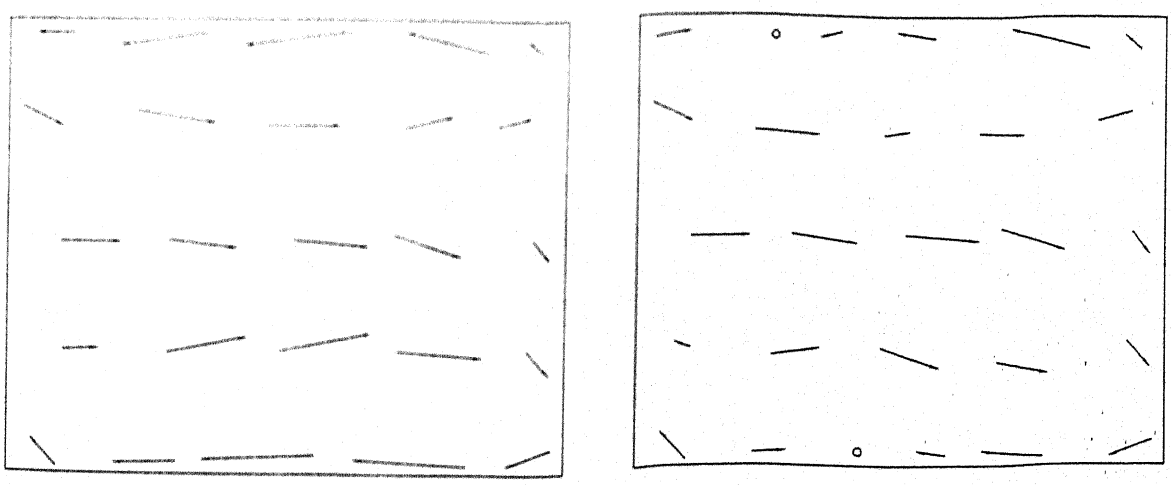

(b) Without fences (a) With fences

Fig. 10 Transverse velocity distribution at diffuser (R/r=6) exit

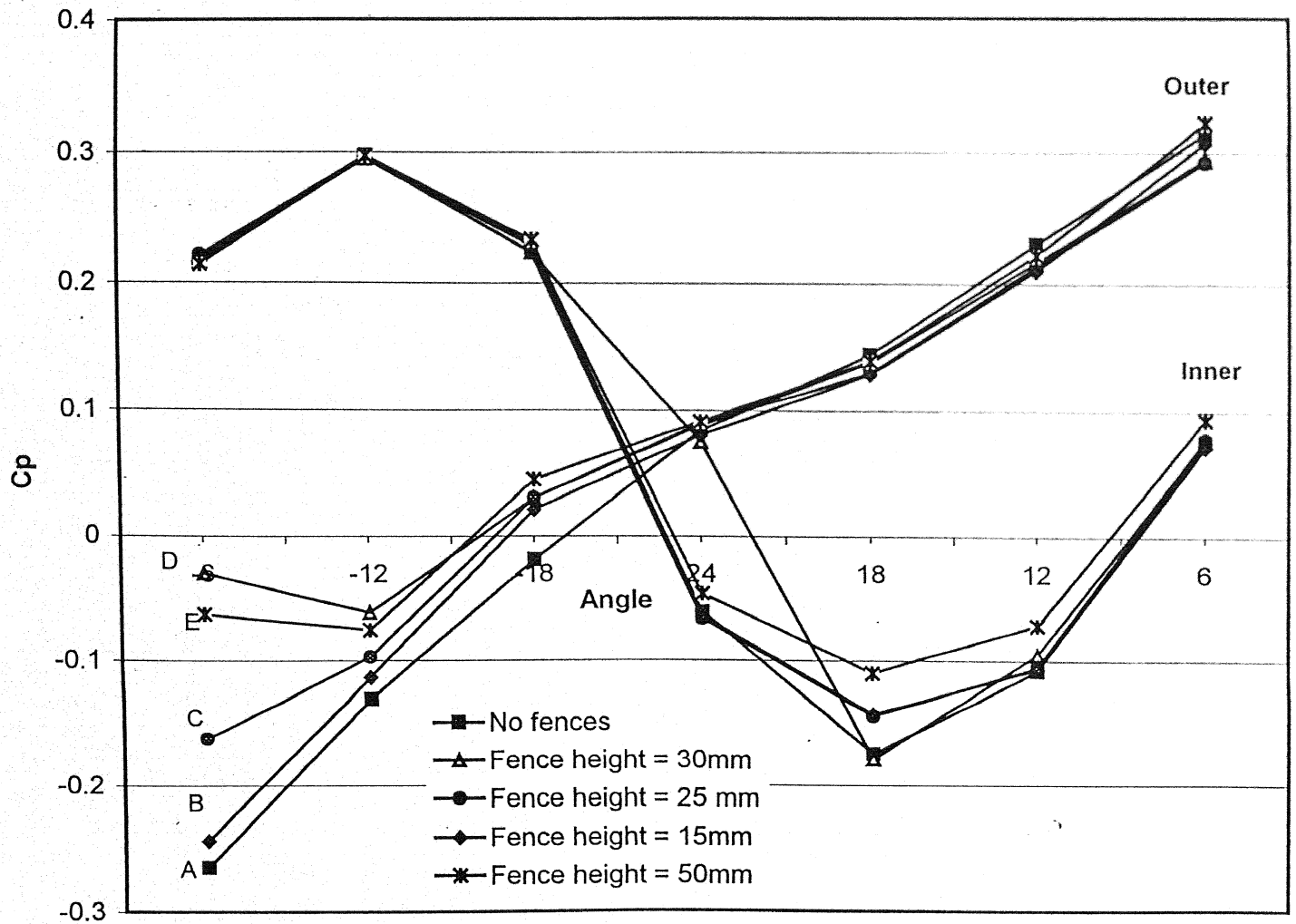

Fig. 11 Outer and inner wall Cp distribution for diffuser2 (R/r=4)

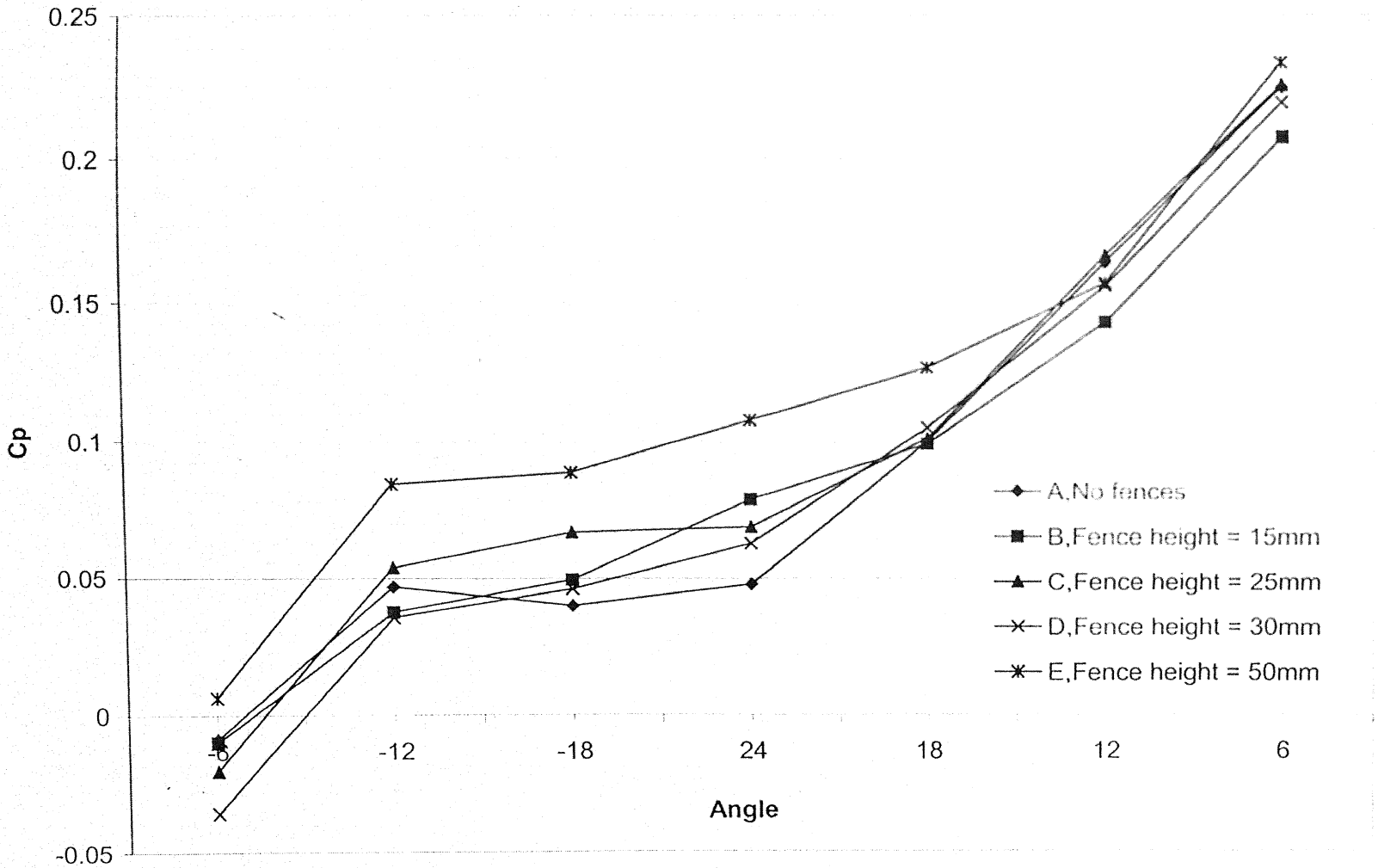

Fig. 12 Centerline Cp distribution for diffuser2 (R/r=4)

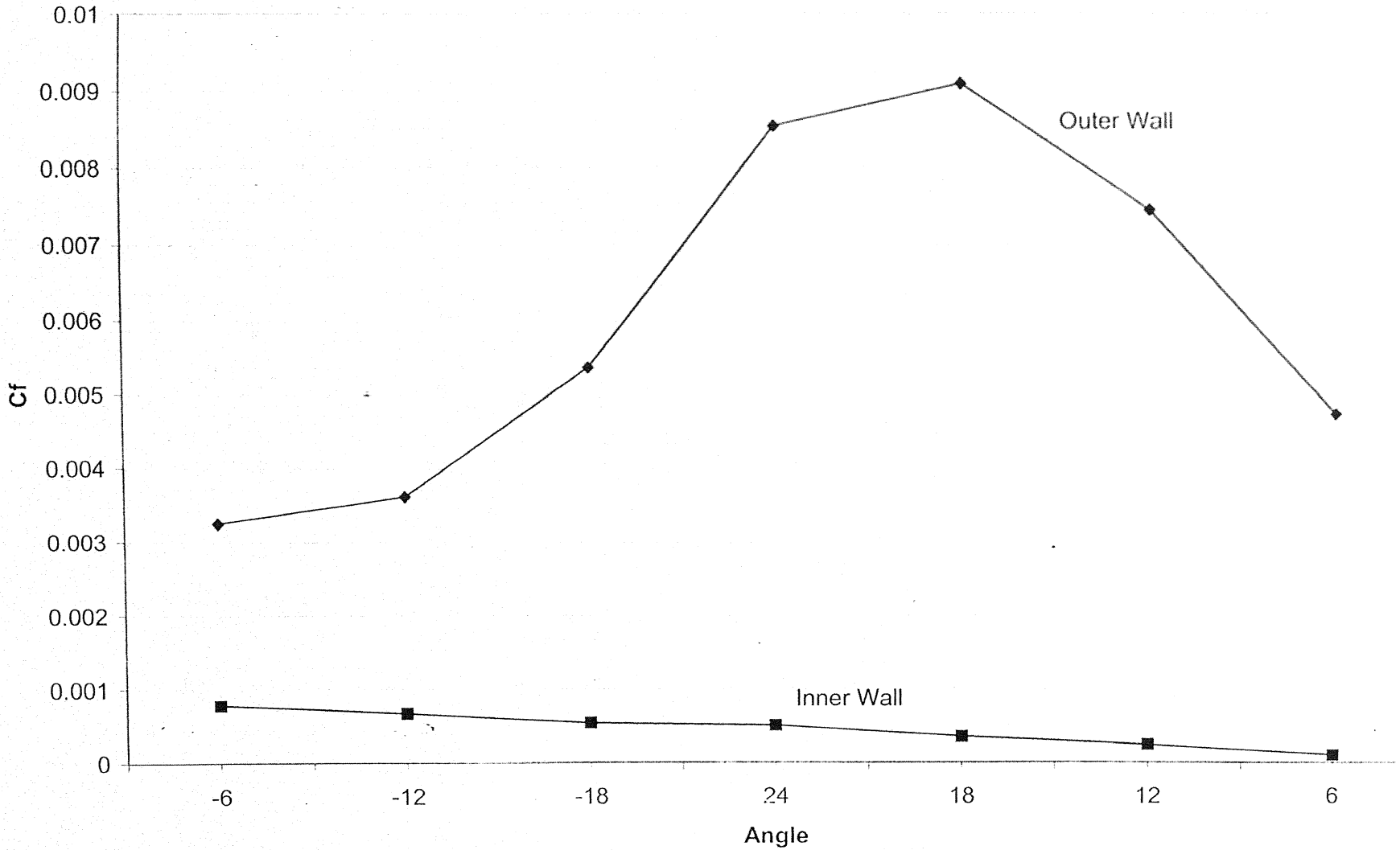

Fig. 13 Skin friction coefficient distribution for diffuser (R/r=4)

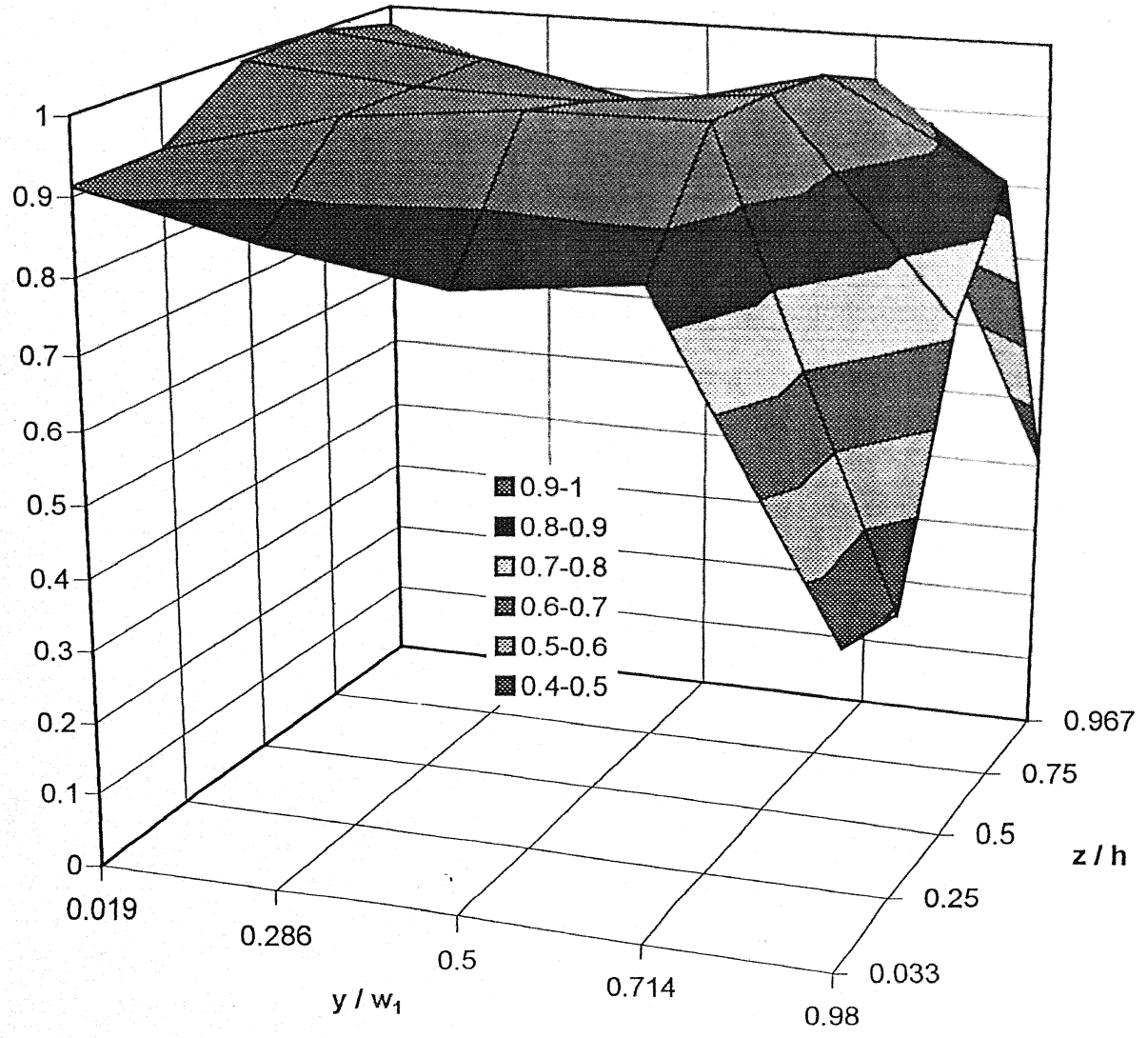

Fig. 14 Velocity distribution at the inflection plane of diffuser2 (R/r=4)

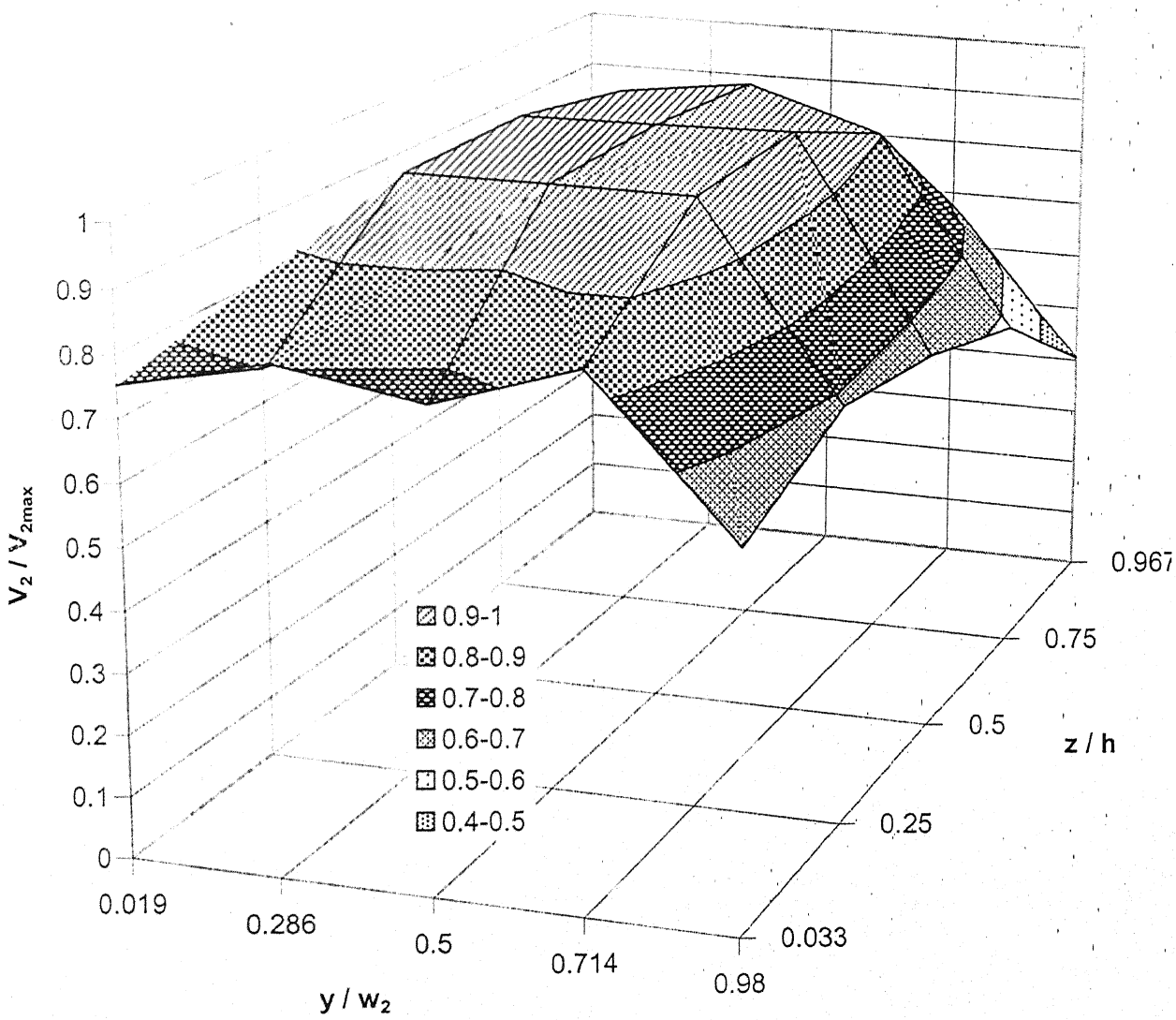

Fig. 15(a) Velocity distribution at diffuser (R/r=4) exit

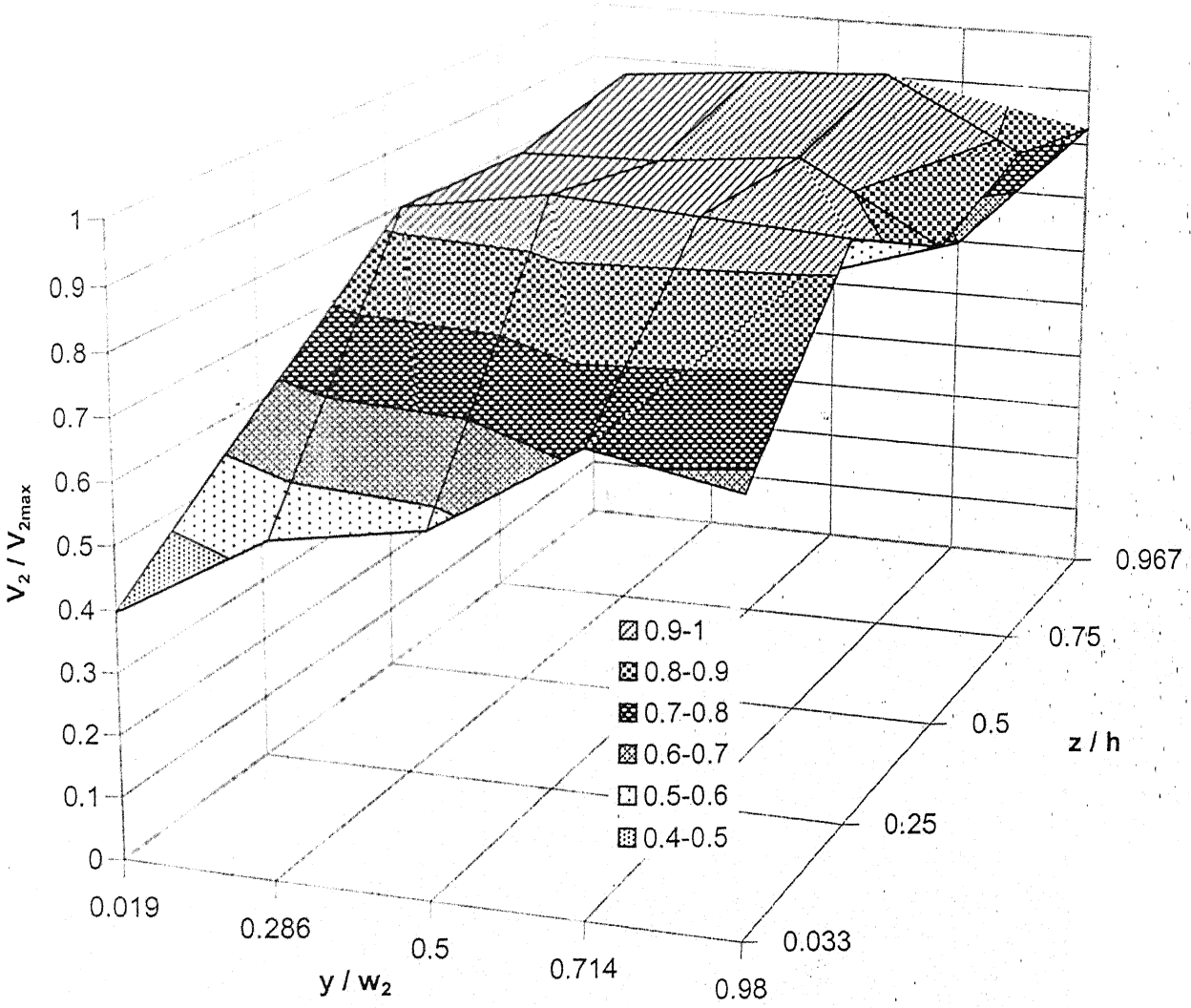

Fig. 15(b) Velocity distribution at diffuser (R/r=4) exit with fences

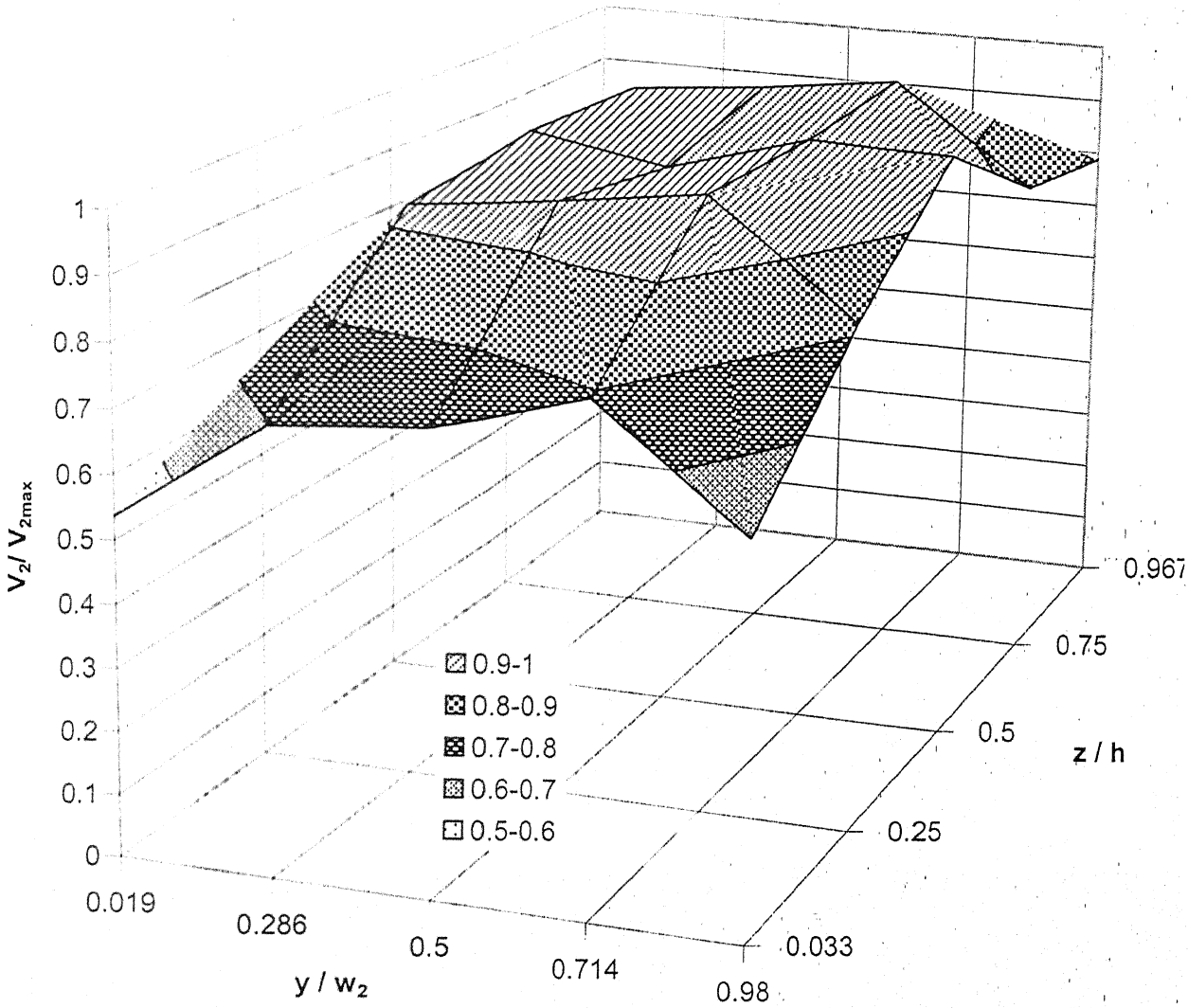

Fig. 15(c) Velocity distribution at diffuser exit (R/r=4) with vortex generator

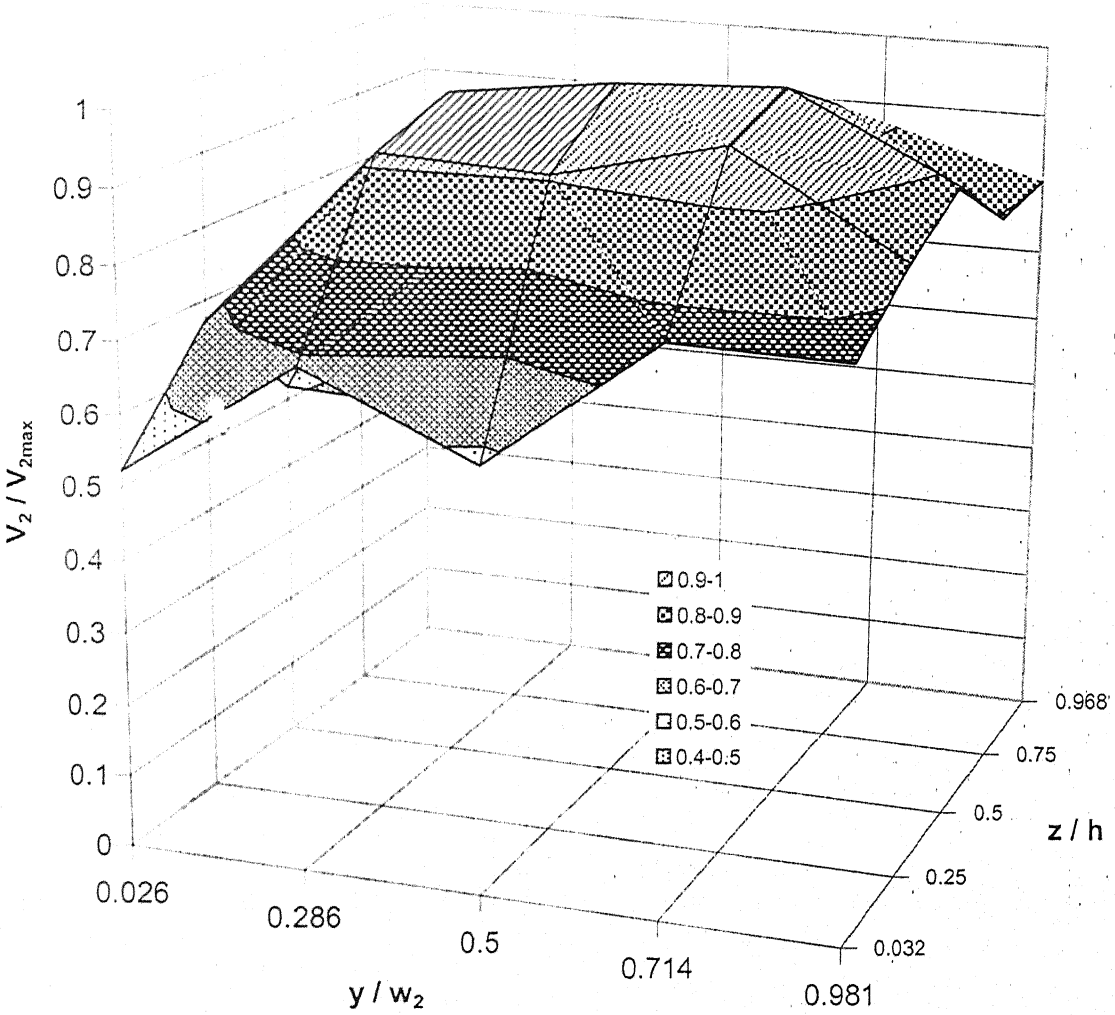

Fig. 15(d) Velocity distribution at diffuser exit (R/r=4) with fences and VG

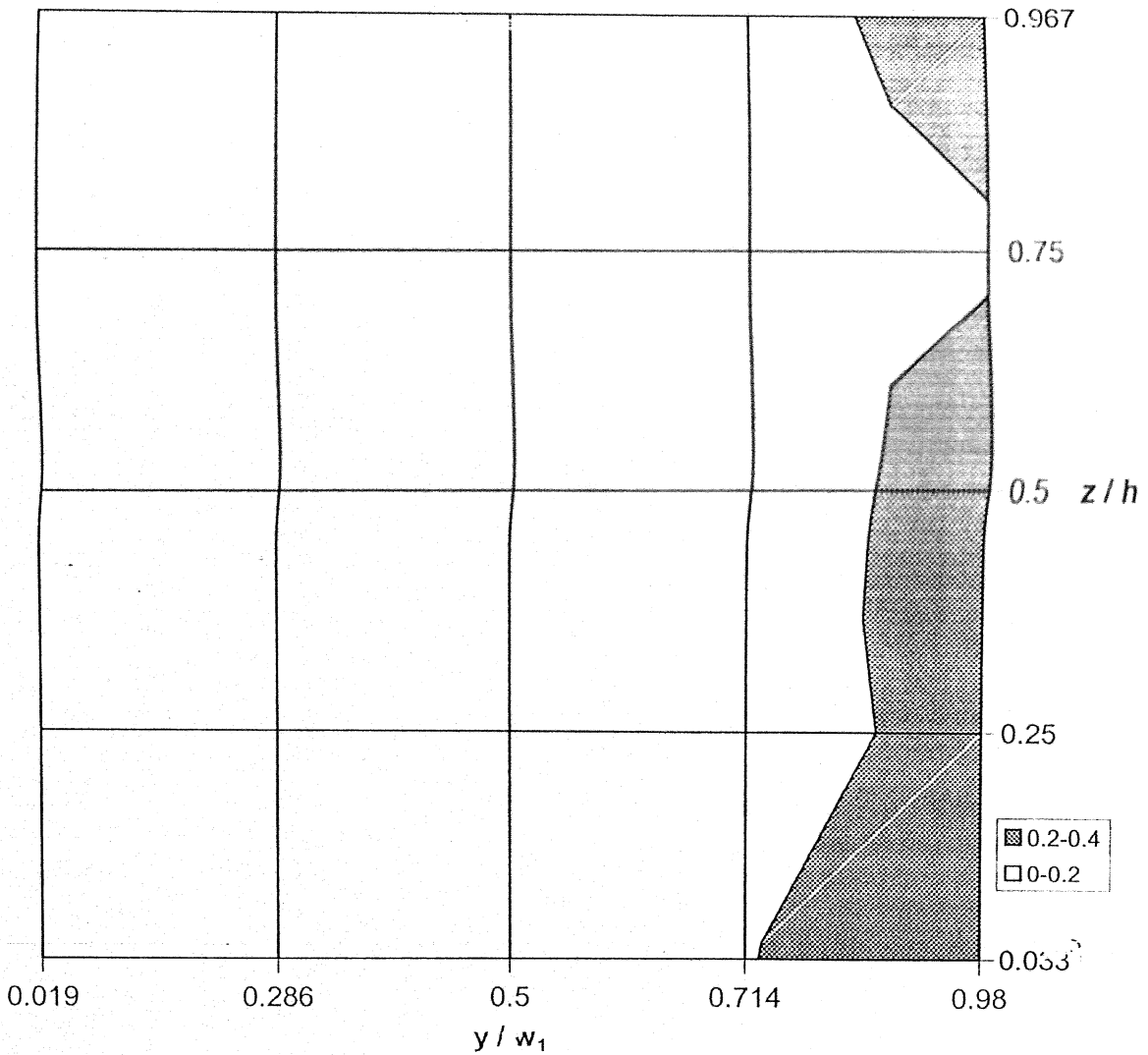

Fig. 16 Loss coefficient distribution at the inflection plane for diffuser2 (R/r=4)

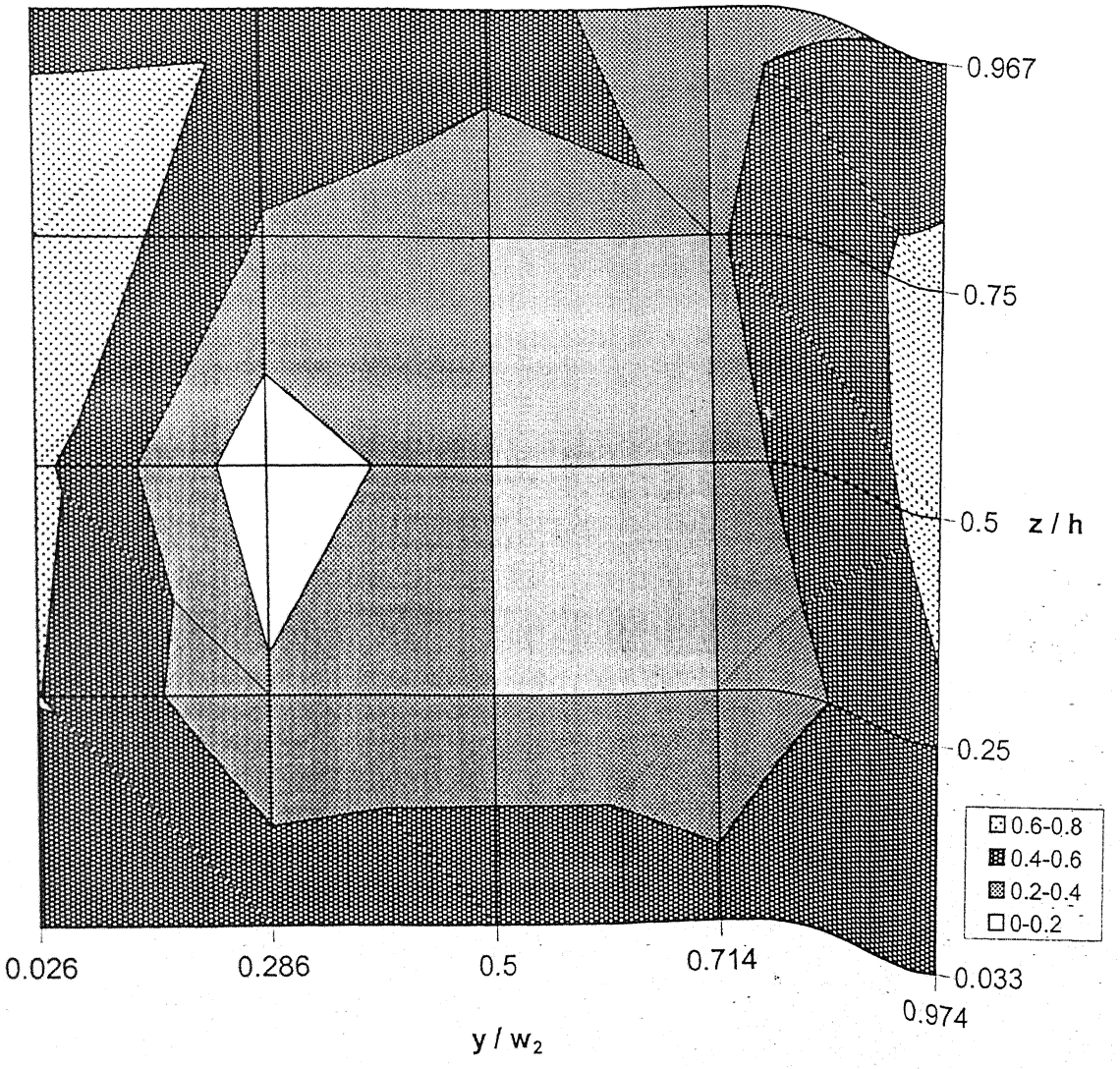

Fig. 17(a) Toatal pressure loss coefficient distribution for bare duct

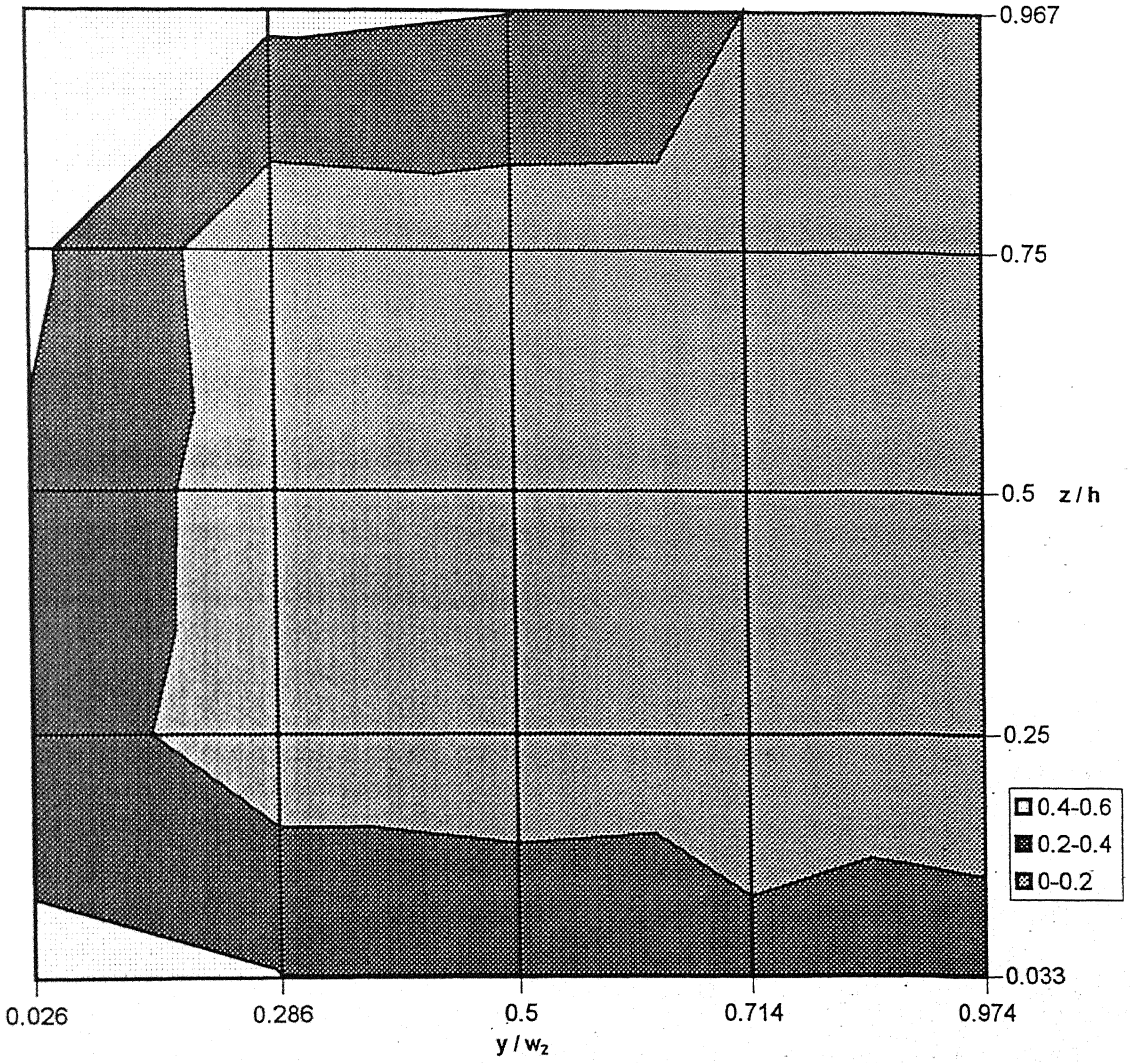

Fig. 17(b) Loss coefficient distribution at diffuser2 (R/r=4) exit with fences

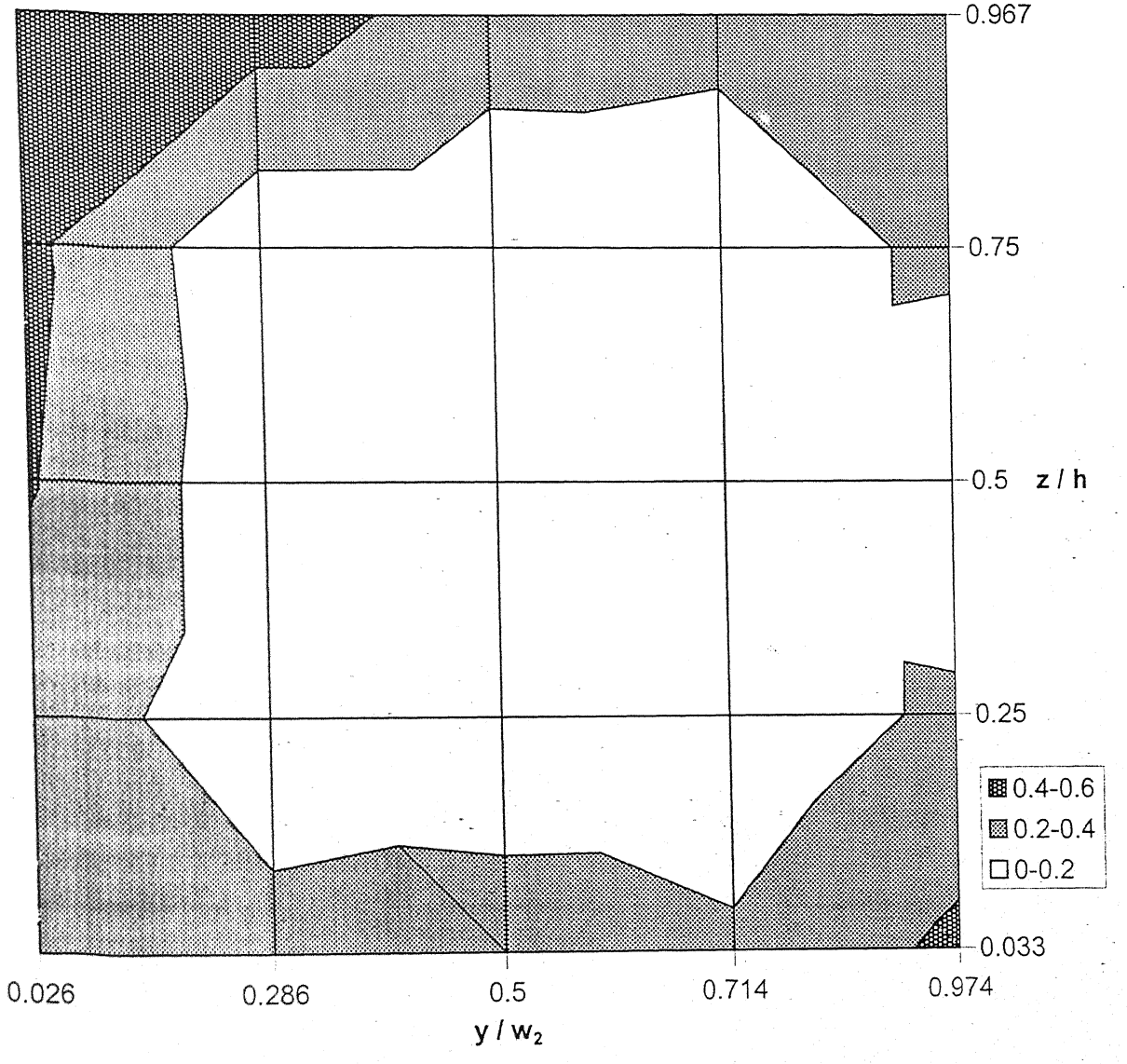

Fig. 17(c) Loss coefficient distribution at diffuser2 (R/r=4) exit with VG

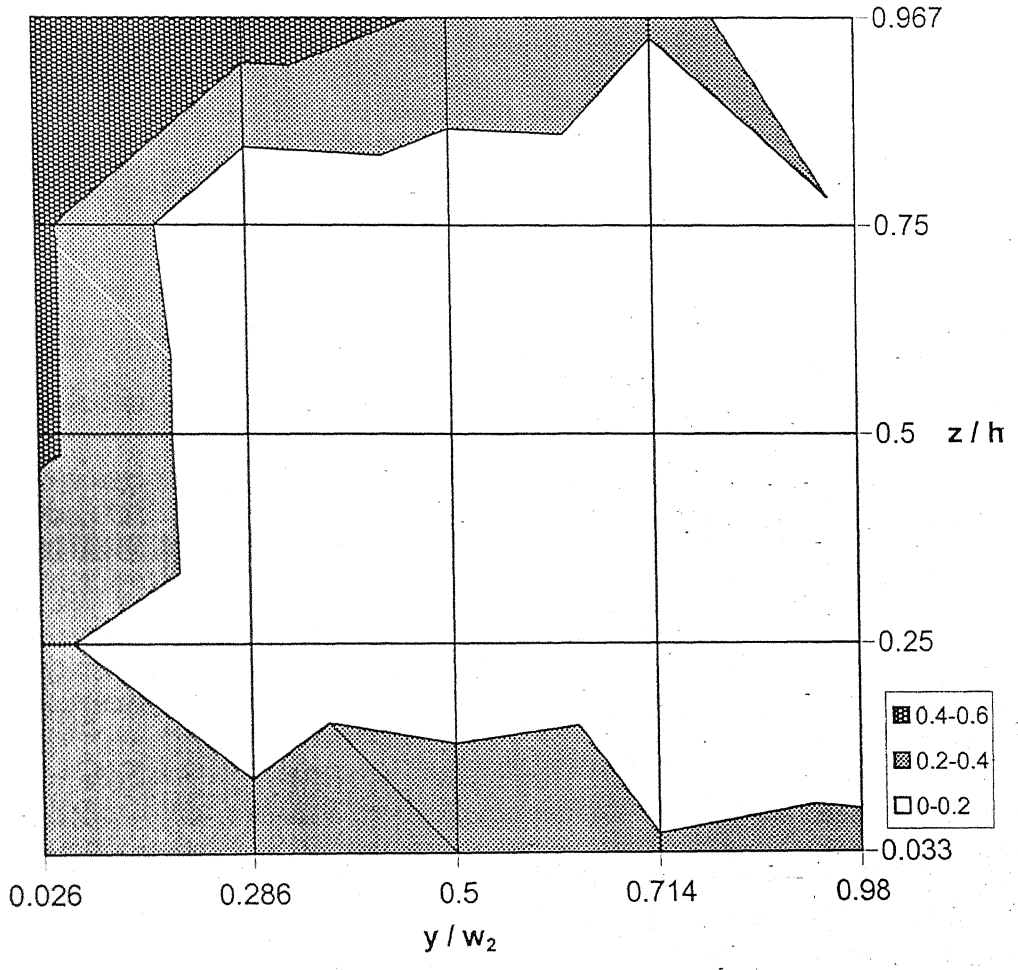

Fig. 17(d) Loss coefficient distribution at diffuser exit with VG and fences

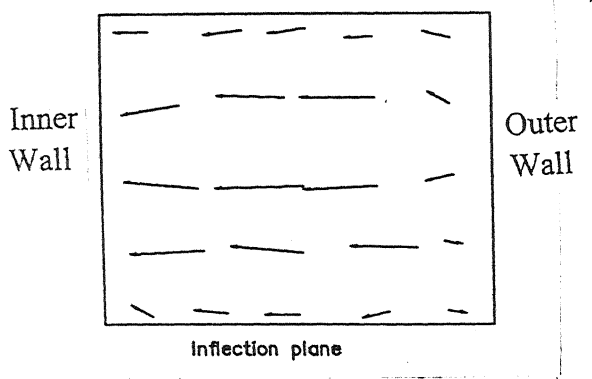

Fig. 18 Transverse velocity distribution at inflection plane

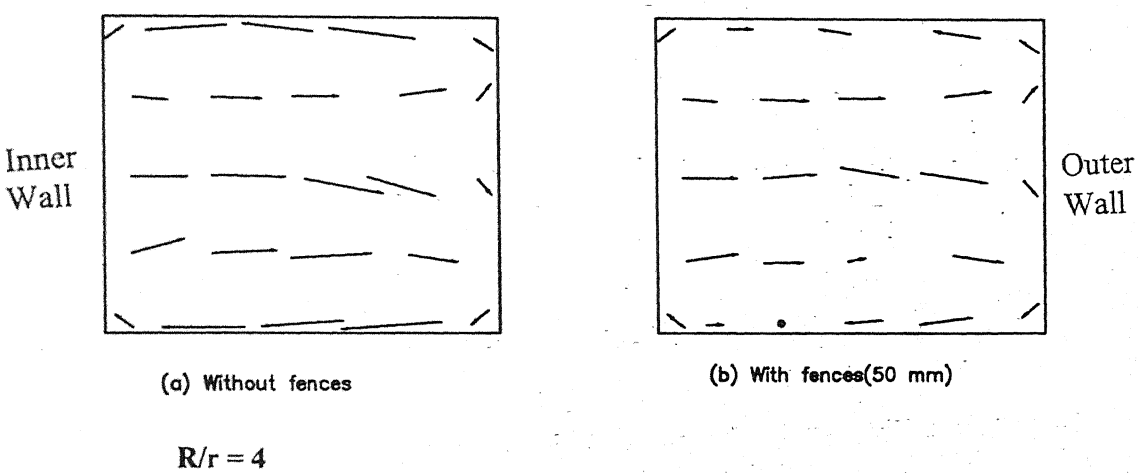

Fig. 19 Transverse velocity distribution at diffuser exit plane

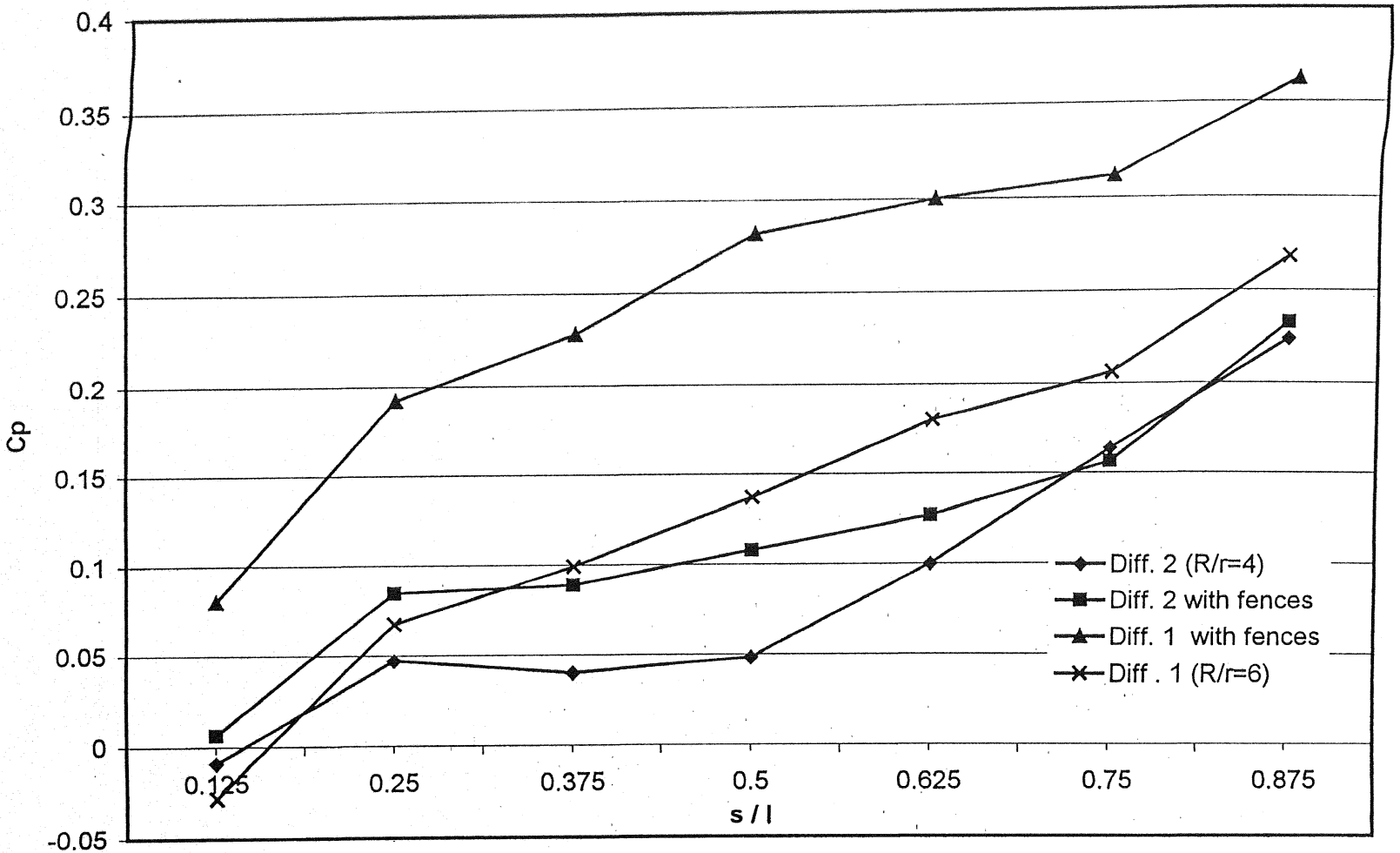

Fig. 20 Comparision of centerline Cp distribution for the two diffusers

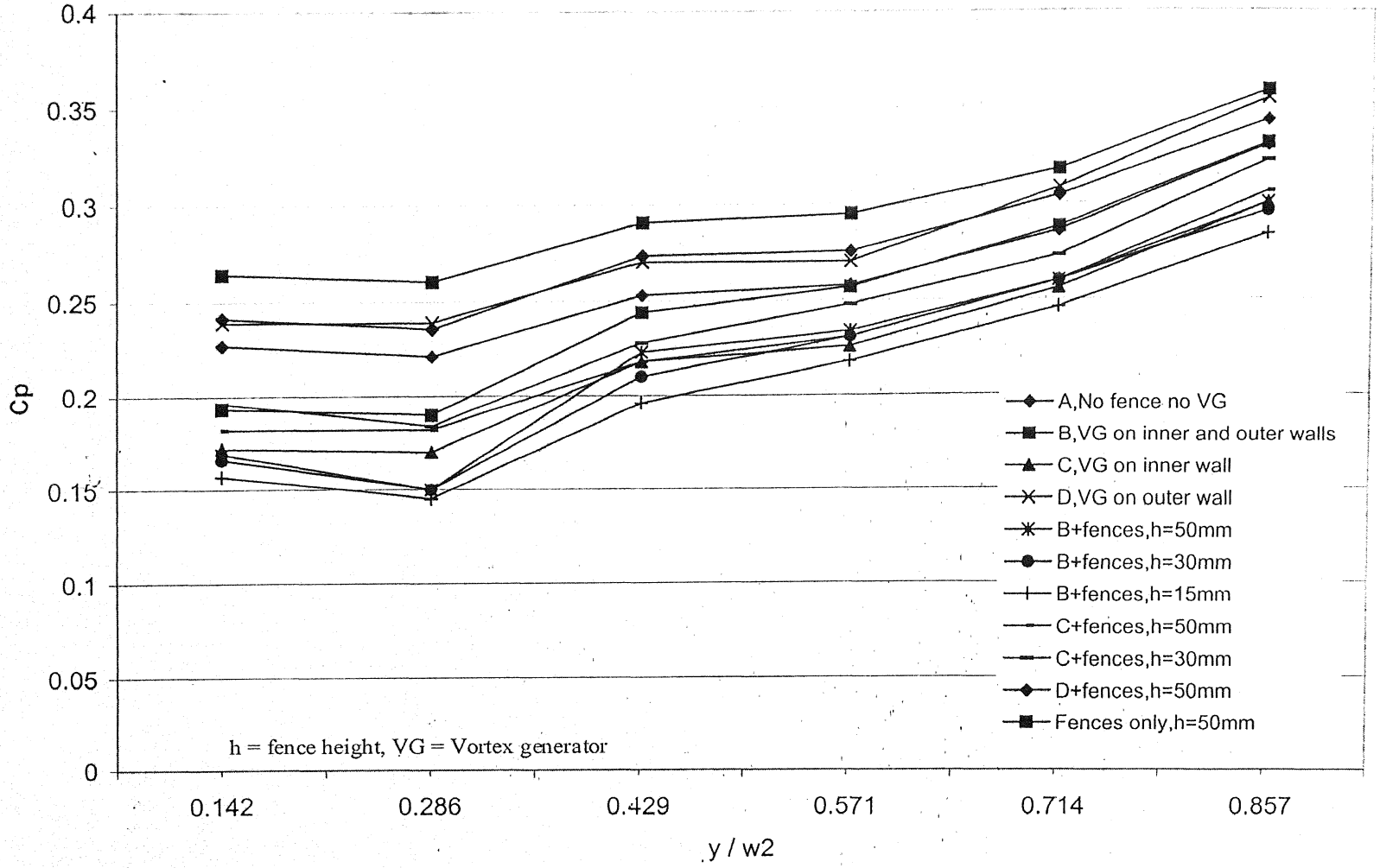

Fig. 21 Cp distribution at the diffuser (R/r=4) exit